

## Supplementary Data

### Molecular design of silane-bridged phosphorus-containing compounds and their flame retardant mechanisms, toughened, water absorption and low dielectric epoxy thermosets

Muhammad Salman <sup>a</sup>, Rukhsana Ashraf <sup>a</sup>, Ze-Tao Xiao <sup>a</sup>, Hao-Jie Shi <sup>a</sup>, Aksam Abdelkhalik <sup>b</sup>,  
Yuan Hu <sup>a</sup>, Xin Wang <sup>a,\*</sup>

<sup>a</sup> State Key Laboratory of Fire Science, University of Science and Technology of China, 96  
Jinzhai Road, Hefei, Anhui 230026, P. R. China.

<sup>b</sup> National Institute of Standards, El-sadat Street, El-Haram, El-Giza, PO Box 136, code  
12211, Egypt

\* Corresponding author. E-mail address: wxcmx@ustc.edu.cn (X. Wang)

#### List of Figures

<b>Figure S1:</b> <sup>1</sup> H-NMR of FR <sub>1</sub> .	6
<b>Figure S2:</b> <sup>31</sup> P-NMR of FR <sub>1</sub> .	6
<b>Figure S3:</b> <sup>29</sup> Si-NMR of FR <sub>1</sub> .	7
<b>Figure S4:</b> HRMS spectrum of FR <sub>1</sub> .	7
<b>Figure S5:</b> FTIR spectra of bDMVSiB, DOPO and FR <sub>1</sub> .	8
<b>Figure S6:</b> <sup>1</sup> H-NMR of FR <sub>2</sub> .	9
<b>Figure S7:</b> <sup>31</sup> P-NMR of FR <sub>2</sub> .	9
<b>Figure S8:</b> <sup>29</sup> Si-NMR of FR <sub>2</sub> .	10
<b>Figure S9:</b> HRMS spectrum of FR <sub>2</sub> .	10
<b>Figure S10:</b> FTIR spectra of bDMVSiB, DPPO and FR <sub>2</sub> .	11
<b>Figure S11:</b> <sup>1</sup> H-NMR of FR <sub>3</sub> .	12
<b>Figure S12:</b> <sup>31</sup> P-NMR of FR <sub>3</sub> .	12
<b>Figure S13:</b> <sup>29</sup> Si-NMR spectrum of FR <sub>3</sub> .	13
<b>Figure S14:</b> HRMS spectrum of FR <sub>3</sub> .	13
<b>Figure S15:</b> FTIR spectra of TMDVSiO, DPPO and FR <sub>3</sub> .	14
<b>Figure S16:</b> TGA and DTG curves under air atmosphere of FR <sub>1</sub> (a, b), FR <sub>2</sub> (c, d) and FR <sub>3</sub> (e, f) respectively.	15
<b>Figure S17:</b> Tensile and impact strengths of different epoxy composites.	16
<b>Figure S18:</b> Comparison of the dielectric constant at 1 MHz frequency of the EP/FR composites of present work with the related literature.	16
<b>Figure S19:</b> Real time digital photos of UL-94 vertical burning test of pure EP thermoset.	17
<b>Figure S20:</b> Real time digital photos of UL-94 vertical burning test of FR <sub>1</sub> epoxy thermosets at different P-content.	18
<b>Figure S21:</b> Real time digital photos of UL-94 vertical burning test of FR <sub>2</sub> epoxy thermosets at different P-content.	19

<b>Figure S22:</b> Real time digital photos of UL-94 vertical burning test of FR <sub>3</sub> epoxy thermosets at different P-content. ....	20
<b>Figure S23:</b> Comparison of MCC curves of pure EP with FR <sub>1</sub> (a), FR <sub>2</sub> (b), and FR <sub>3</sub> (c) epoxy thermosets at different phosphorous content. ....	21
<b>Figure S24:</b> (a) C <sub>1s</sub> , (b) N <sub>1s</sub> and (c) O <sub>1s</sub> , XPS spectra for the char residue of EP. ....	21
<b>Figure S25:</b> (a) C <sub>1s</sub> , (b) N <sub>1s</sub> and (c) O <sub>1s</sub> , (d) Si <sub>2p</sub> and (e) P <sub>2p</sub> XPS spectra for the char residue of EP/FR <sub>2</sub> -0.25P. ....	22
<b>Figure S26:</b> (a) C <sub>1s</sub> , (b) N <sub>1s</sub> and (c) O <sub>1s</sub> , (d) Si <sub>2p</sub> and (e) P <sub>2p</sub> XPS spectra for the char residue of EP/FR <sub>3</sub> -0.25P. ....	22
<b>Figure S27:</b> 3D TG-IR spectra of gaseous pyrolysis volatiles of (a) EP, (b) EP/FR <sub>1</sub> -0.25P, (c) EP/FR <sub>2</sub> -0.25P and (d) EP/FR <sub>3</sub> -0.25P. ....	23
<b>Figure S28:</b> Comparison of TIC curve of EP and EP/FR <sub>1</sub> -0.25P, EP/FR <sub>2</sub> -0.25P, EP/FR <sub>3</sub> -0.25P composites. ....	24
<b>Figure S29:</b> TIC curve along with the mass spectra of different fragments at their respective retention time and proposed pyrolysis pathway of the FR <sub>2</sub> . ....	25
<b>Figure S30:</b> TIC curve along with the mass spectra of different fragments at their respective retention time and proposed pyrolysis pathway of the FR <sub>3</sub> . ....	25

### List of Tables

<b>Table S1:</b> TGA data of designed epoxy thermosets under air atmosphere. ....	26
<b>Table S2:</b> DMA results of epoxy thermosets. ....	26
<b>Table S3:</b> Tensile strength and impact strength of epoxy thermoset in previous research. ....	27
<b>Table S4:</b> Comparison of the dielectric constant at 1 MHz frequency for different epoxy thermosets in present work and other related literature. ....	27
<b>Table S5:</b> Flame retardancy performance of the designed EP thermosets through cone calorimetry. ....	28
<b>Table S6:</b> Identification of typical pyrolysis products for EP obtained from Py-GC/MS. ....	28
<b>Table S7:</b> Identification of typical pyrolysis products for EP/FR <sub>1</sub> -0.25P obtained from Py-GC/MS. ....	29
<b>Table S8:</b> Identification of typical pyrolysis products for EP/FR <sub>2</sub> -0.25P obtained from Py-GC/MS. ....	30
<b>Table S9:</b> Identification of typical pyrolysis products for EP/FR <sub>3</sub> -0.25P obtained from Py-GC/MS. ....	31

## Characterization

The nuclear magnetic resonance (NMR) spectra for protons, silicon, and phosphorus were obtained using a Bruker AVANCE III 400 NMR spectrometer, manufactured in Germany.

Fourier transform infrared (FTIR) spectra were obtained using a Nicolet 6700 spectrometer (Nicolet Instrument Co., USA) employing the KBr disc method. The spectra were recorded with a scanning time of 32, covering a wavenumber range from 4000 to 400  $\text{cm}^{-1}$ .

High-resolution mass spectrometry (HRMS) was conducted with an LTQ-Orbitrap XL electrostatic field orbital trap mass spectrometer (Thermo-Fisher, USA). The samples were dissolved in methanol and tested in positive ion mode.

The thermal decomposition behaviour of the samples was evaluated via a Q5000 thermogravimetric analyzer (TGA) (TA Instruments, USA). The sample (approximately 5.0 mg) was heated from 50 to 800  $^{\circ}\text{C}$  at a ramp rate of 10  $^{\circ}\text{C}/\text{min}$ .

Dynamic mechanical analysis (DMA) was performed using a Q800 instrument (TA Instruments, USA) throughout a temperature range of 25 to 250  $^{\circ}\text{C}$ , with a heating rate of 5  $^{\circ}\text{C}/\text{min}$ . The measurements of the cured samples were 50 mm  $\times$  10 mm  $\times$  3 mm.

The tensile properties were assessed using an electromechanical universal testing equipment (MTS Criterion 43, USA) at a crosshead velocity of 10 mm/min. The mean value derived from a minimum of three repeated measurements was documented. The dimensions of the sample were 100 mm  $\times$  10 mm  $\times$  3 mm.

Differential scanning calorimetry (DSC) was conducted using a DSC Q2000 (TA Instruments Inc., USA) in a nitrogen atmosphere. The glass transition temperature ( $T_g$ ) of the EP composites was determined at a heating rate of 10  $^{\circ}\text{C}/\text{min}$  and noted at the midpoint of the inflection curve during the second heating cycle.

The transmittance of the 1.0 mm thick EP plates was assessed using a Solidspec-3700 UV/vis spectrometer (Japan).

Measurements of the limiting oxygen index (LOI) were conducted using an HC-2 LOI apparatus (Jiangning, China) in accordance with ASTM D2863-97, with sample dimensions of 100 mm  $\times$  5.0 mm  $\times$  3 mm.

The samples' anti-flammability was assessed using a UL-94 vertical burning chamber in accordance with ASTM D3801-10, with dimensions of 125 mm  $\times$  13 mm  $\times$  3 mm.

Cone calorimeter assessments were conducted using a TESTECH cone calorimeter (Suzhou, China) at a heat flux of 50 kW/m<sup>2</sup> in accordance with ISO 5660-1, with sample dimensions of 100 mm × 100 mm × 3 mm.

The measurement of microscale combustion calorimetry (MCC) was conducted utilising a FTT calorimeter designed by Lyon and Walters. Approximately 5 mg of the sample was subjected to heating from 100 to 600 °C at a rate of 60 °C/min under a nitrogen atmosphere, after which the resulting decomposition volatiles were directed to a combustor at 900 °C, where they were mixed with oxygen for complete combustion. The heat release rate was calculated based on the principle of oxygen consumption, and the total heat released was determined by integrating the area under the heat release rate curve.

The morphology of the residues was examined using SU8200 field emission scanning electron microscopy (SEM) (Hitachi, Japan) at an accelerating voltage of 3 kV.

The microstructure of the char residues was analysed using a LabRAM-HR confocal Raman microprobe equipped with a 514.5 nm argon-ion laser.

The elemental composition of the char residues was determined using an ESCALAB 250Xi X-ray photoelectron spectrometer (XPS) from Thermo Fisher Scientific, USA.

Thermogravimetric analysis in conjunction with Fourier transform infrared spectroscopy (TGA-FTIR) was conducted using a Q50 TGA (TA Instruments, USA) linked to an iS50 FTIR instrument (Nicolet, USA) under nitrogen, with a temperature increase from room temperature to 800 °C at a rate of 20 °C/min.

Thermogravimetric analysis-mass spectrometry (TGA-MS) experiments were conducted using a thermogravimetric-infrared chromatography-mass spectrometer (Perkin Elmer Company, USA) to examine the composition and structure of gas phase products during the real-time thermal decomposition of the samples. The samples were subjected to heating in a nitrogen environment, increasing from ambient temperature to 800 °C at a rate of 20 °C/min, utilising electron bombardment ionisation mode for mass spectrometry analysis.

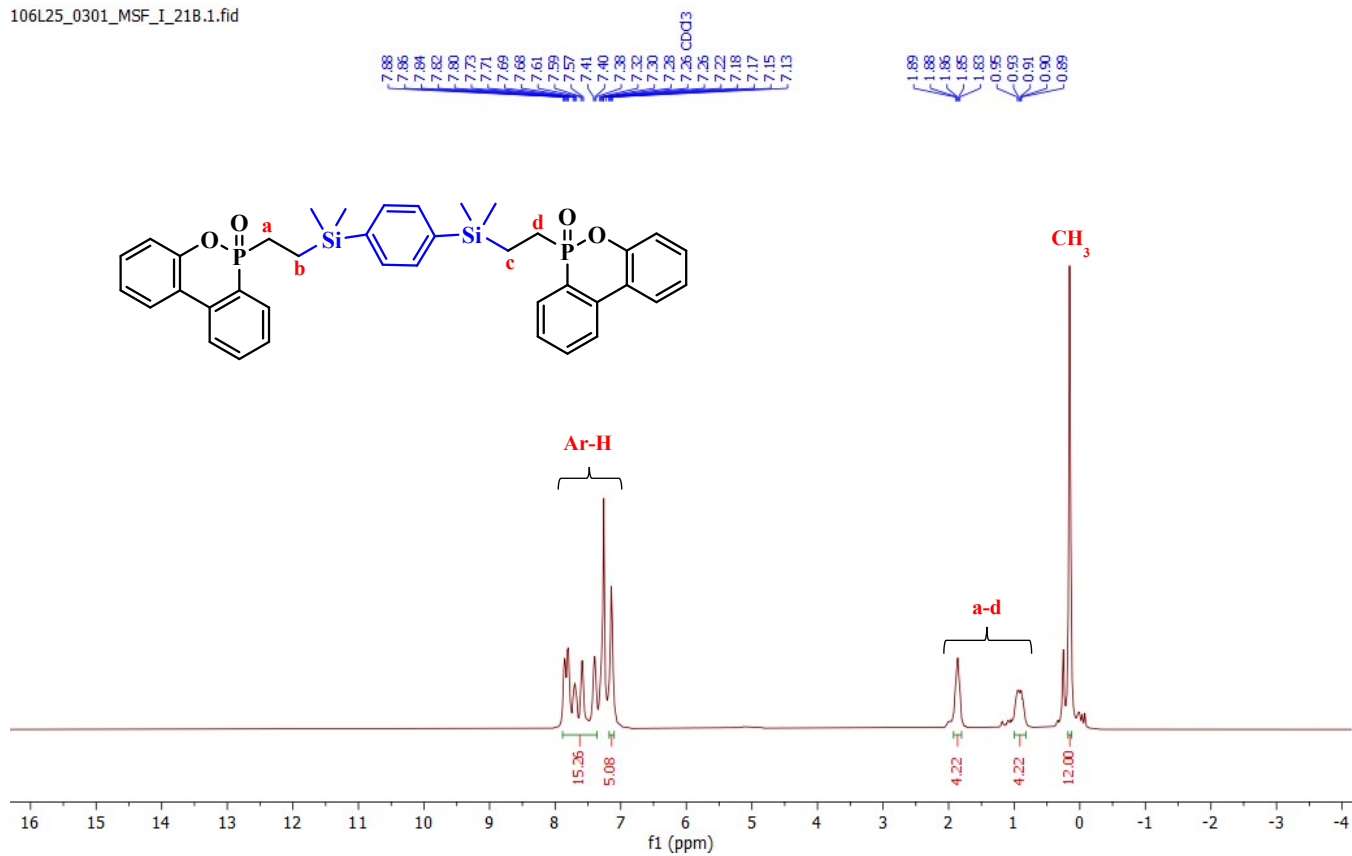
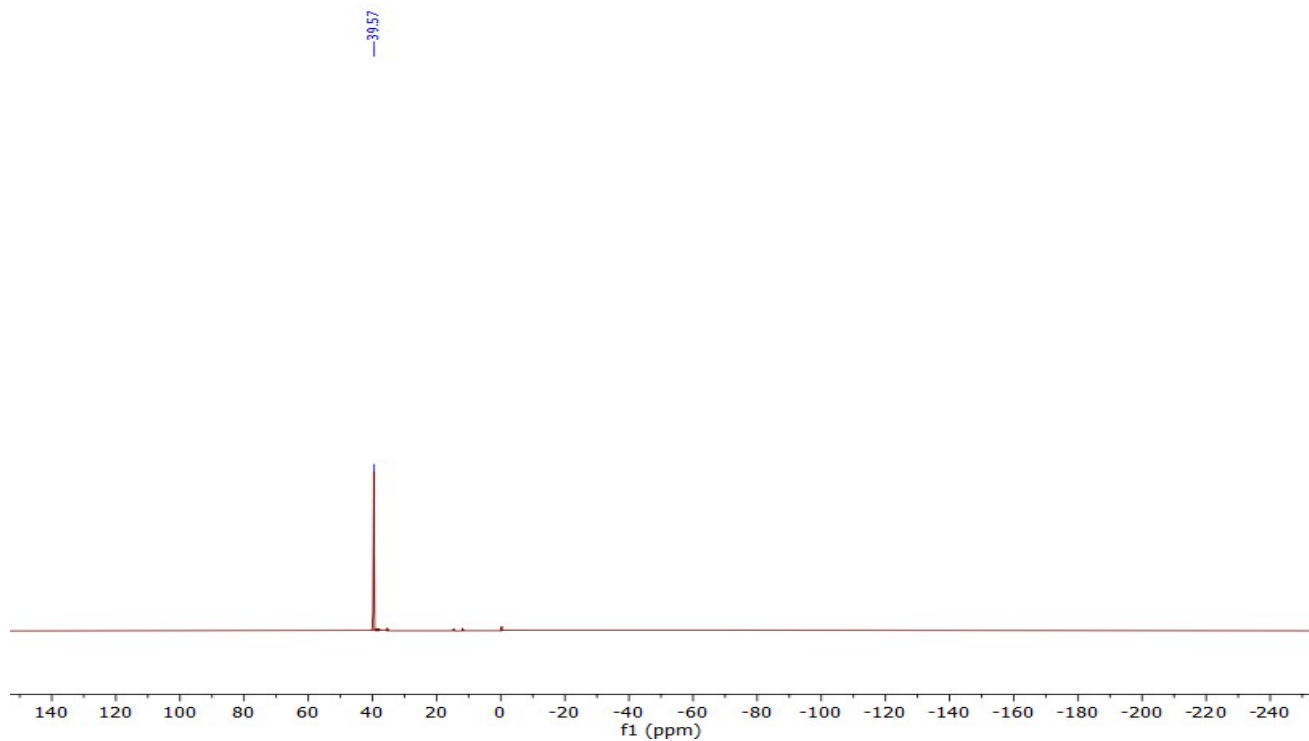
### List of abbreviations

Abbreviation	Full Name
DGEBA	Diglycidyl ether of bisphenol A
DDS	4,4'-Diaminodiphenyl sulfone

---

<b>EP</b>	Epoxy thermoset (pure DGEBA/DDS system)
<b>EPFR<sub>n</sub>-mP</b>	Epoxy thermoset with FR <sub>n</sub> i.e. n= 1, 2, 3 at m wt% phosphorus content i.e. m= 0.25, 0.5, 0.75 wt%
<b>FR<sub>1</sub></b>	DOPO-bDMVSiB phosphorus-silicon flame retardant 1
<b>FR<sub>2</sub></b>	DPPO-bDMVSiB phosphorus-silicon flame retardant 2
<b>FR<sub>3</sub></b>	DOPO-TMDVSiO phosphorus-silicon flame retardant 3
<b>bDMVSiB</b>	1,4-Bisdimethylvinylsilylbenzene
<b>TMDVSiO</b>	1,1,3,3-Tetramethyl-1,3-divinyldisiloxane
<b>DPPO</b>	Diphenyl phosphine oxide
<b>DOPO</b>	6H-Dibenz[c,e] oxaphosphinine 6-oxide
<b>LOI</b>	Limiting oxygen index
<b>UL-94</b>	UL-94 vertical burning test
<b>TTI</b>	Time to ignition
<b>PHRR</b>	Peak heat release rate
<b>THR</b>	Total heat release
<b>TSP</b>	Total smoke production
<b>av-EHC</b>	Average effective heat of combustion
<b>FRI</b>	Flame retardant index
<b>T<sub>5%</sub></b>	Temperature at 5% weight loss
<b>T<sub>max</sub></b>	Temperature at maximum degradation rate
<b>R<sub>max</sub></b>	Maximum degradation rate
<b>T<sub>g</sub></b>	Glass transition temperature
<b>DMA</b>	Dynamic mechanical analysis
<b>E'</b>	Storage modulus
<b>tan δ</b>	Loss tangent
<b>v<sub>e</sub></b>	Crosslinking density
<b>DC</b>	Dielectric constant
<b>DL</b>	Dielectric loss

---

**Figure S1:** <sup>1</sup>H-NMR of FR<sub>1</sub>.**Figure S2:** <sup>31</sup>P-NMR of FR<sub>1</sub>.

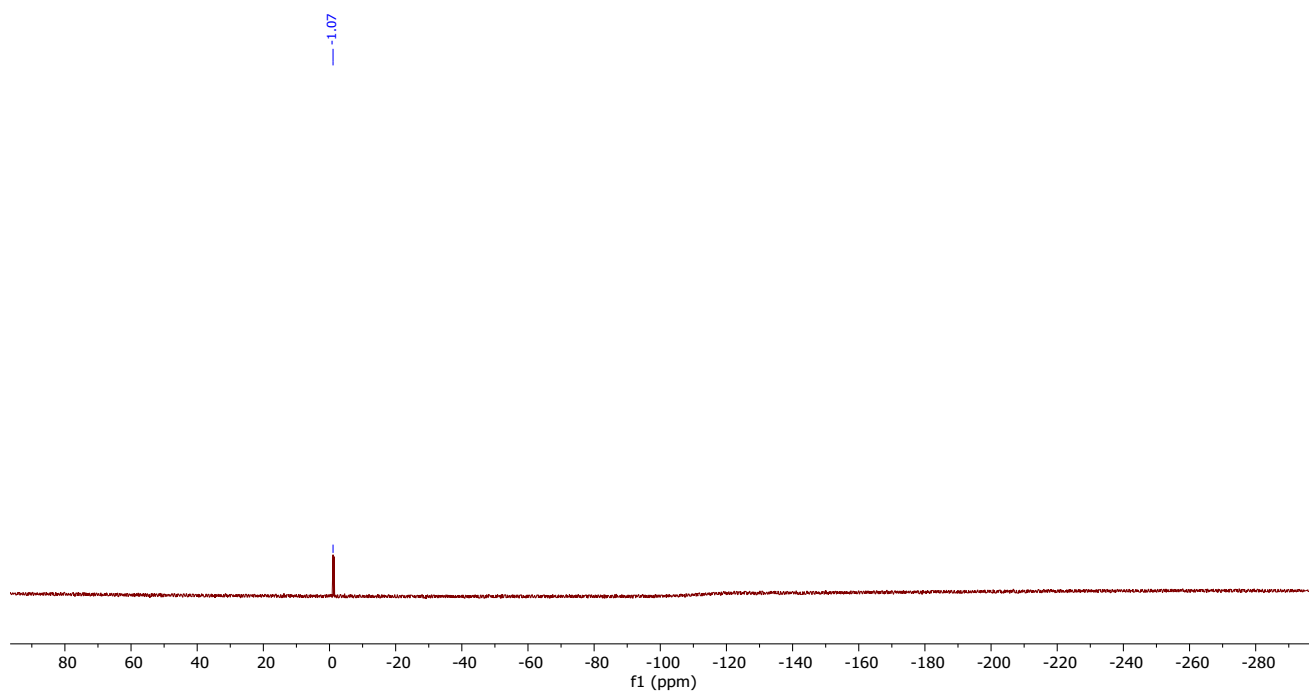


**Figure S3:**  $^{29}\text{Si}$ -NMR of  $\text{FR}_1$ .

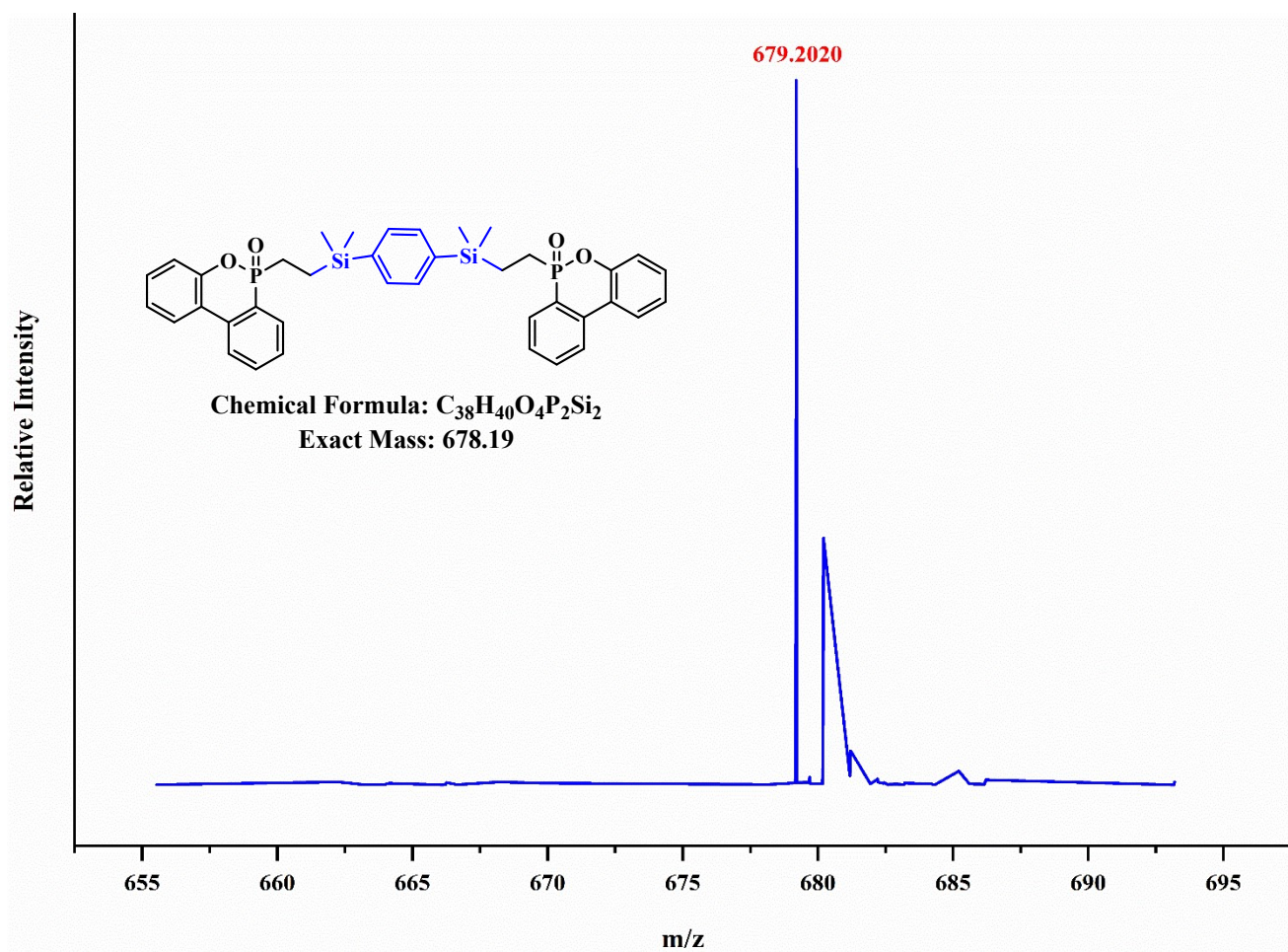


**Figure S4:** HRMS spectrum of  $\text{FR}_1$ .

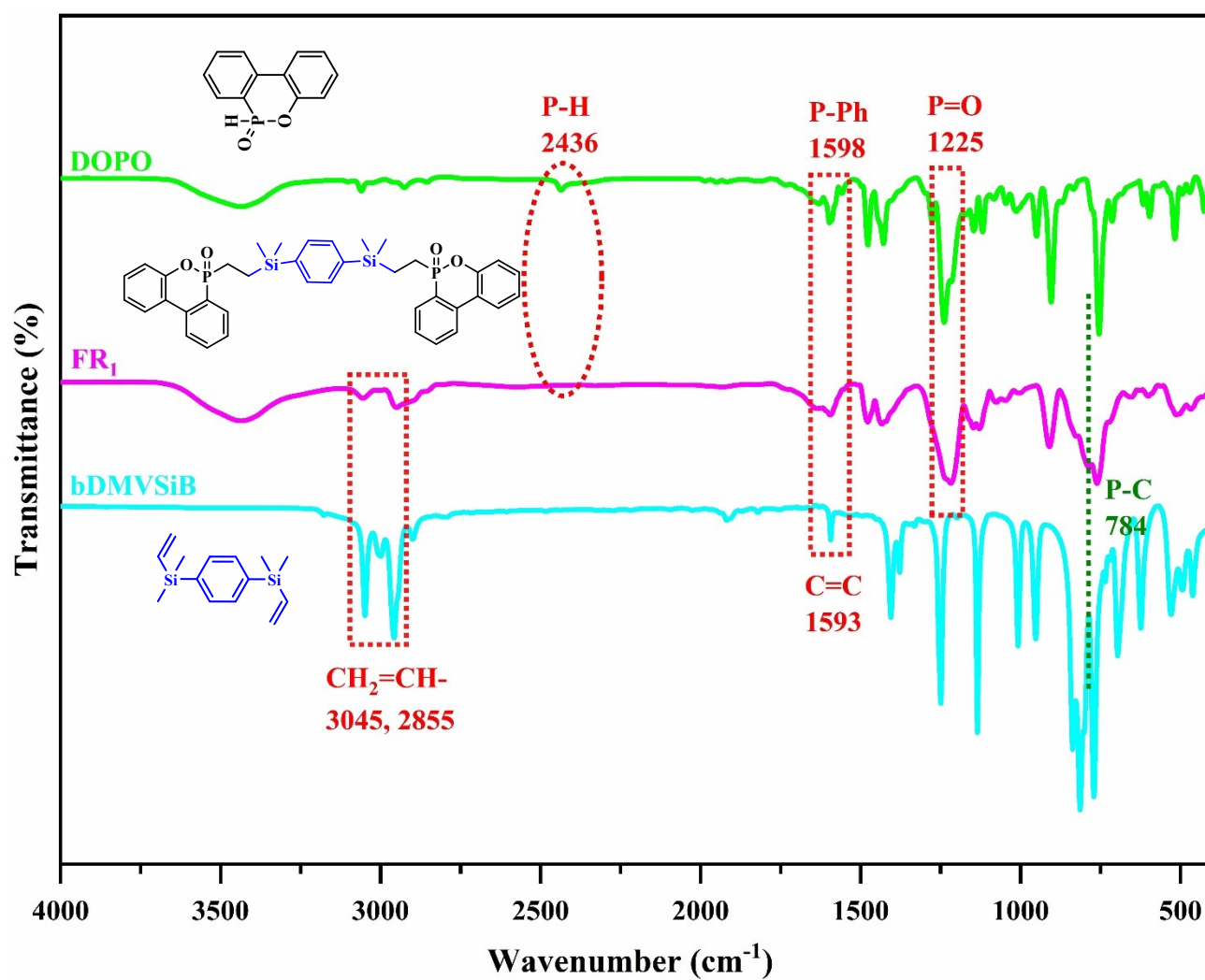
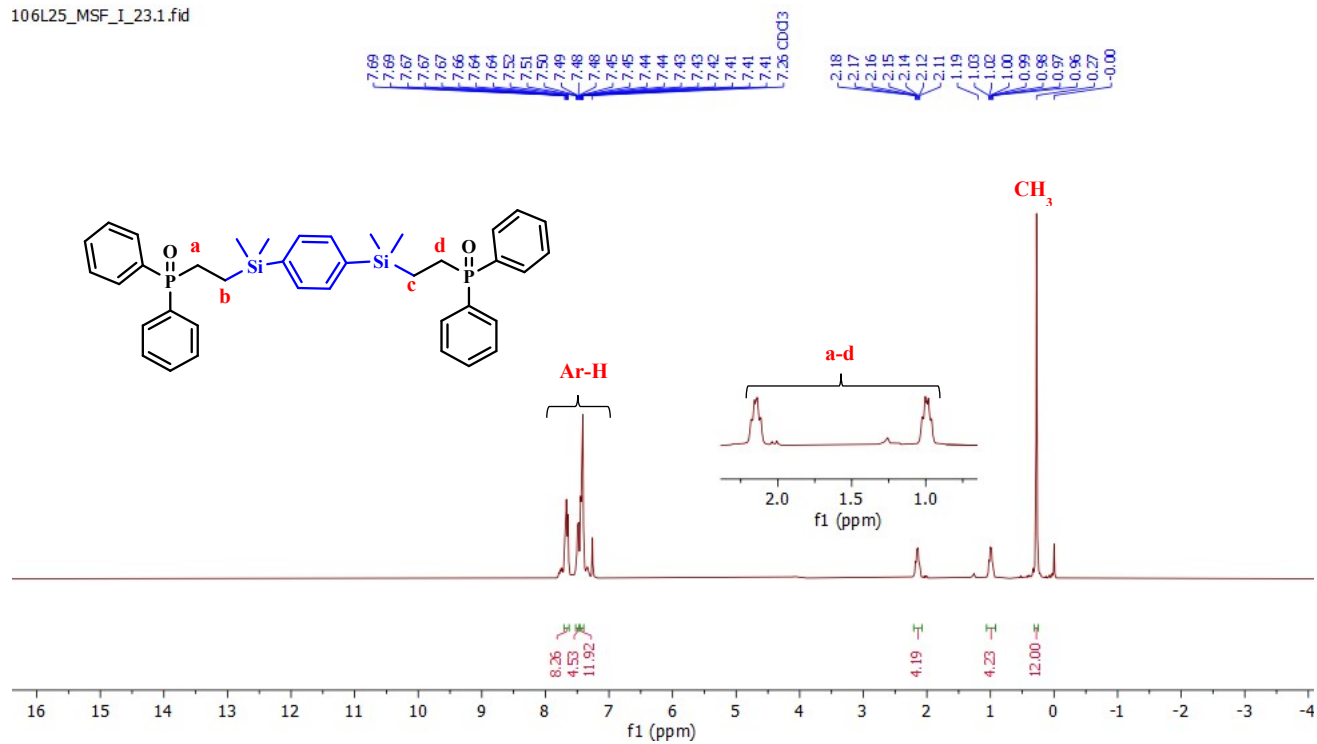
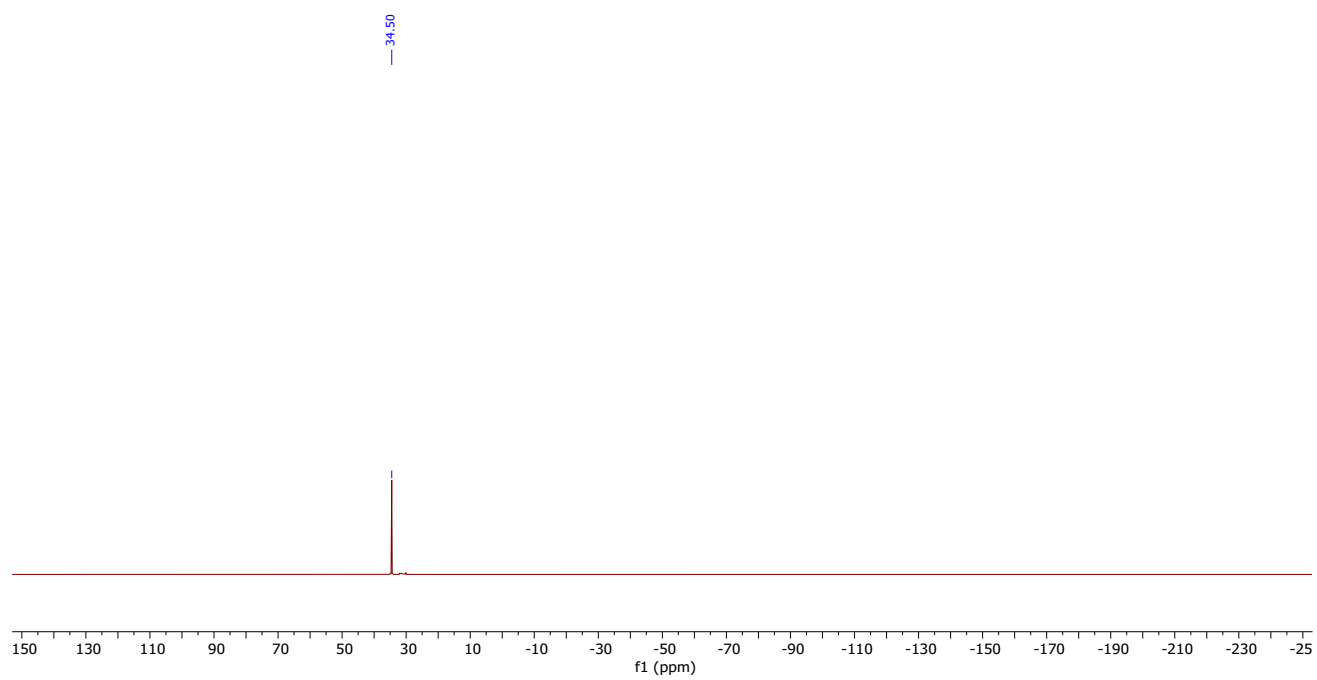
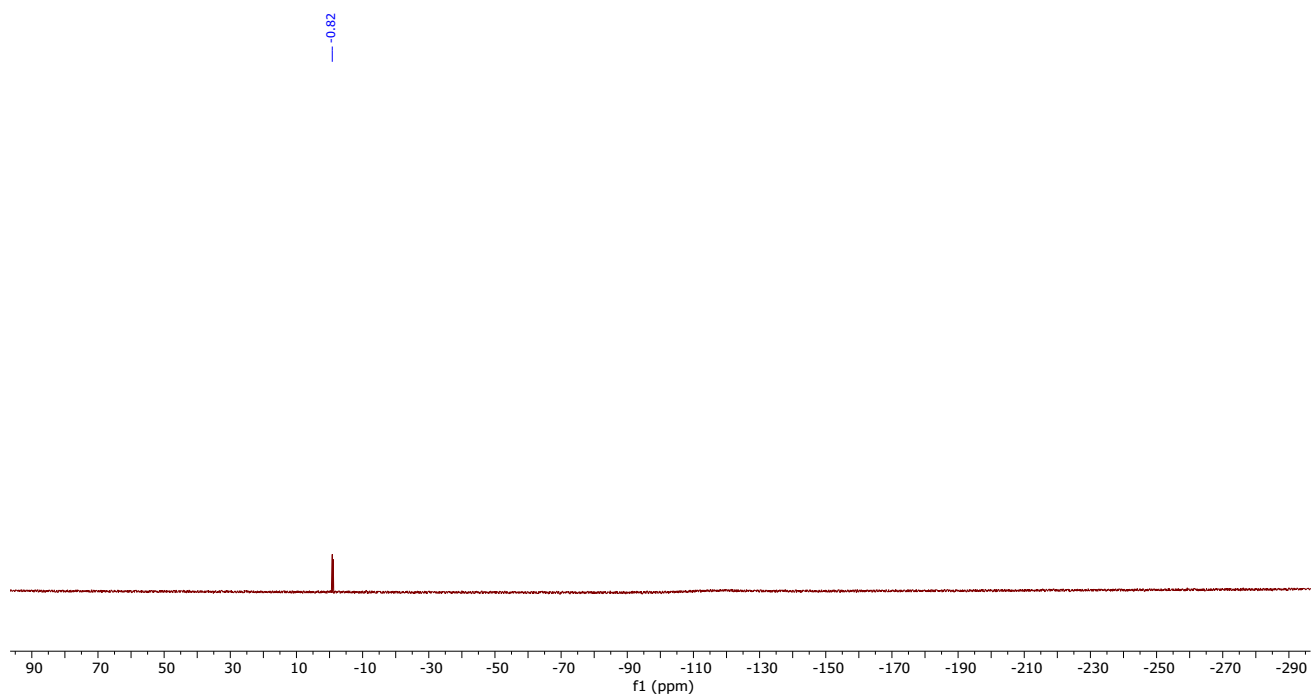
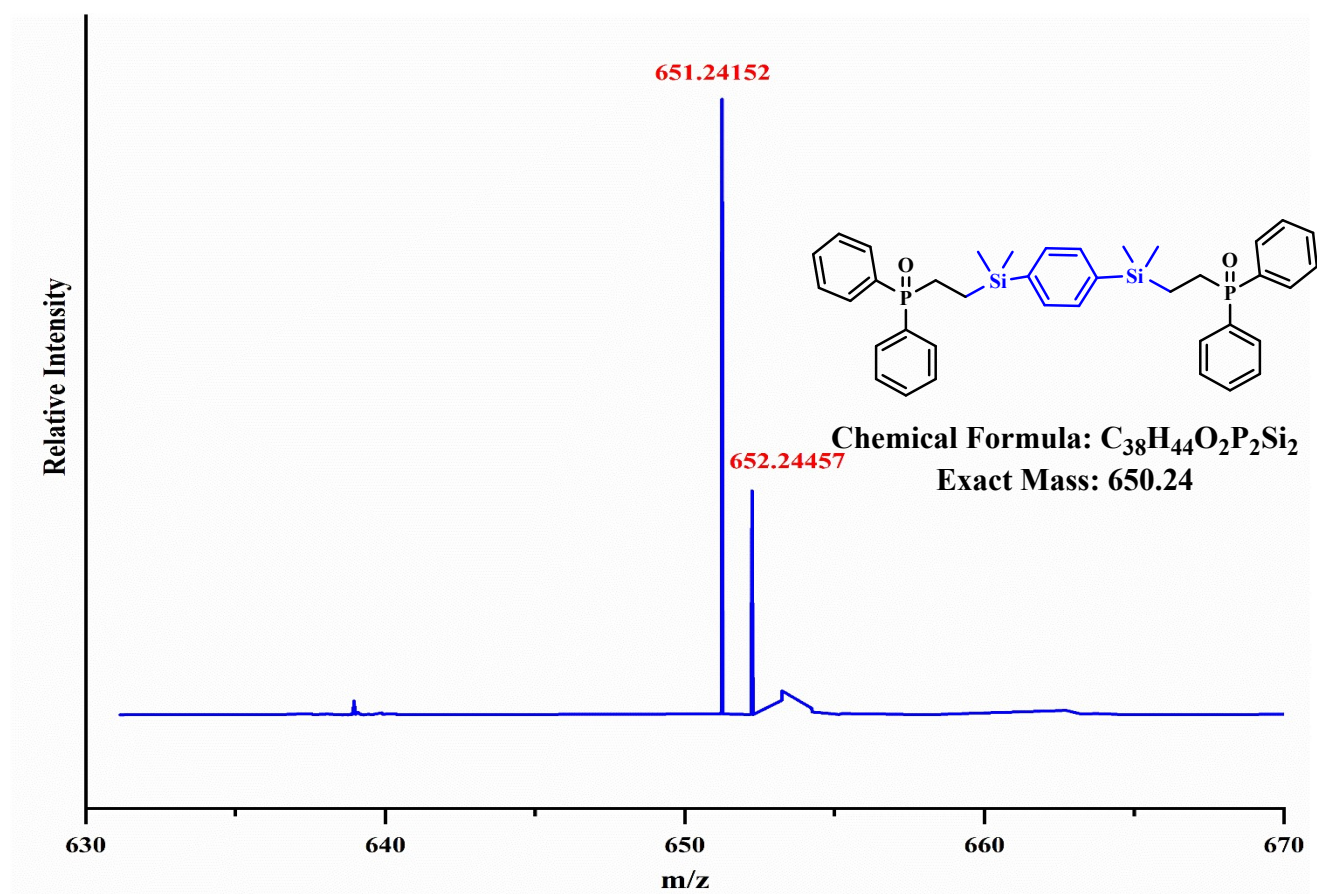


Figure S5: FTIR spectra of bDMVSiB, DOPO and FR<sub>1</sub>.

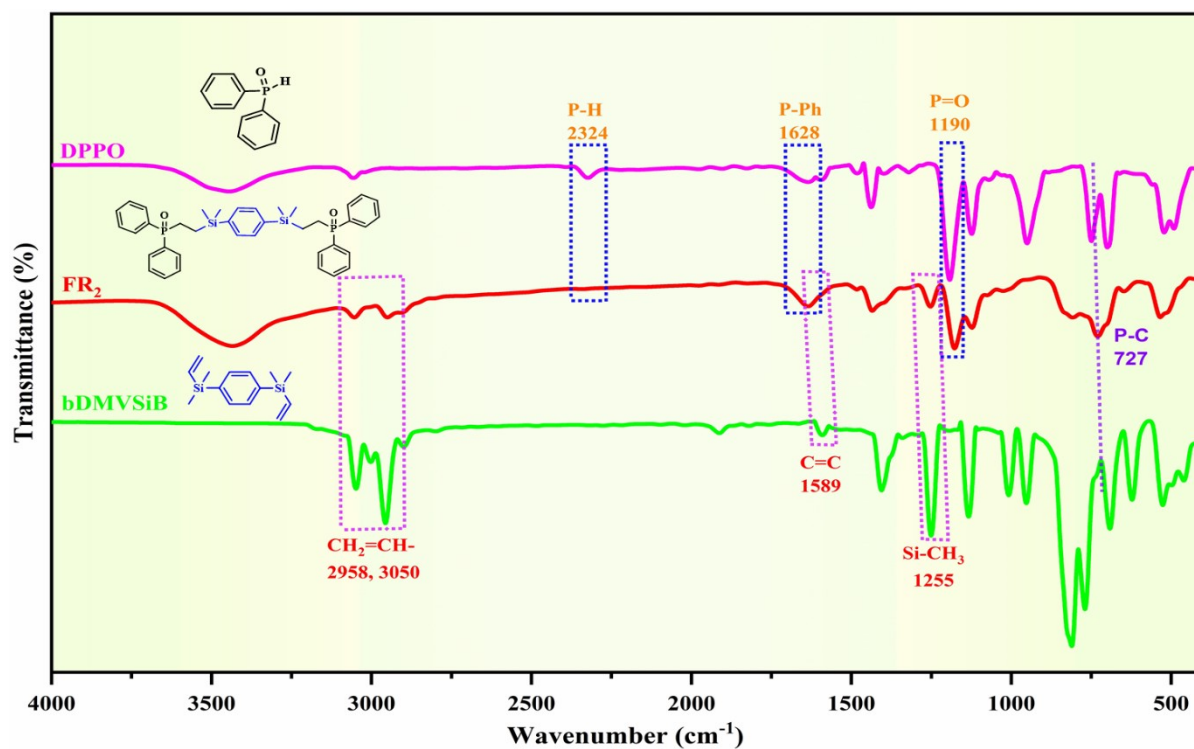
Figure S6: <sup>1</sup>H-NMR of FR<sub>2</sub>.Figure S7: <sup>31</sup>P-NMR of FR<sub>2</sub>.



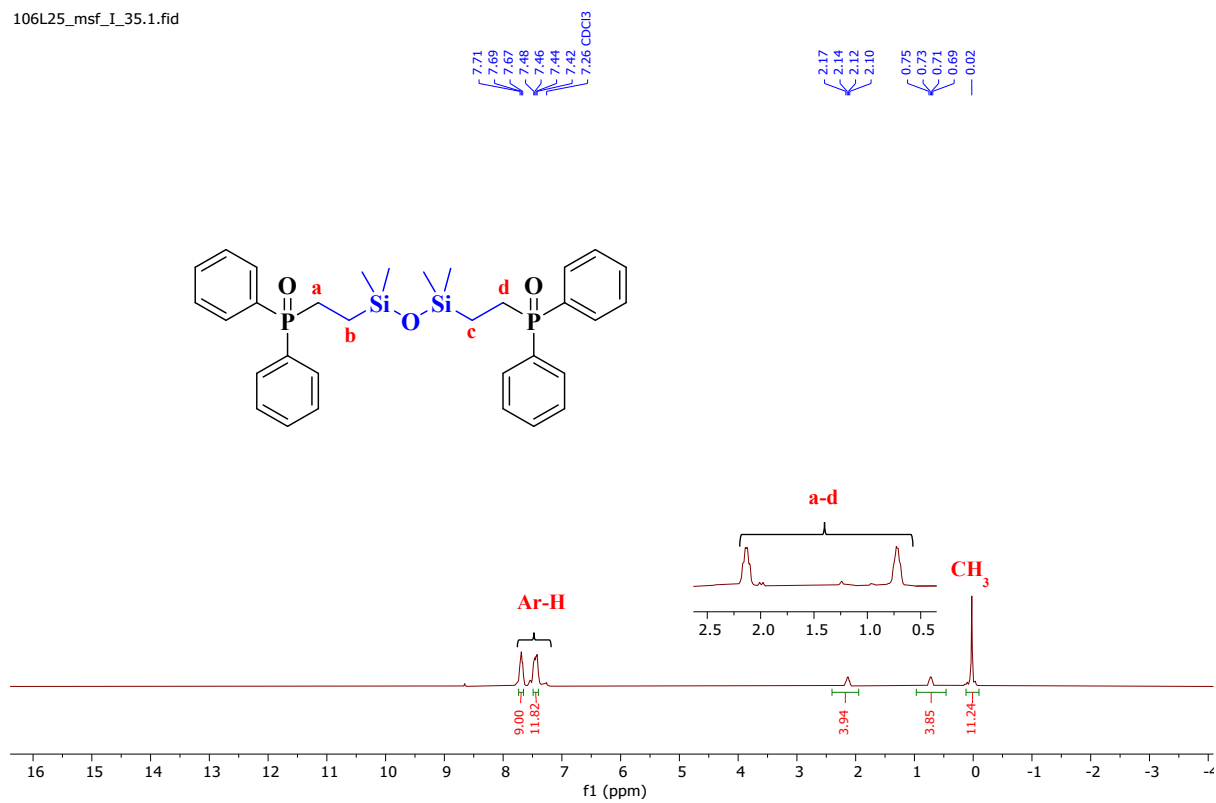
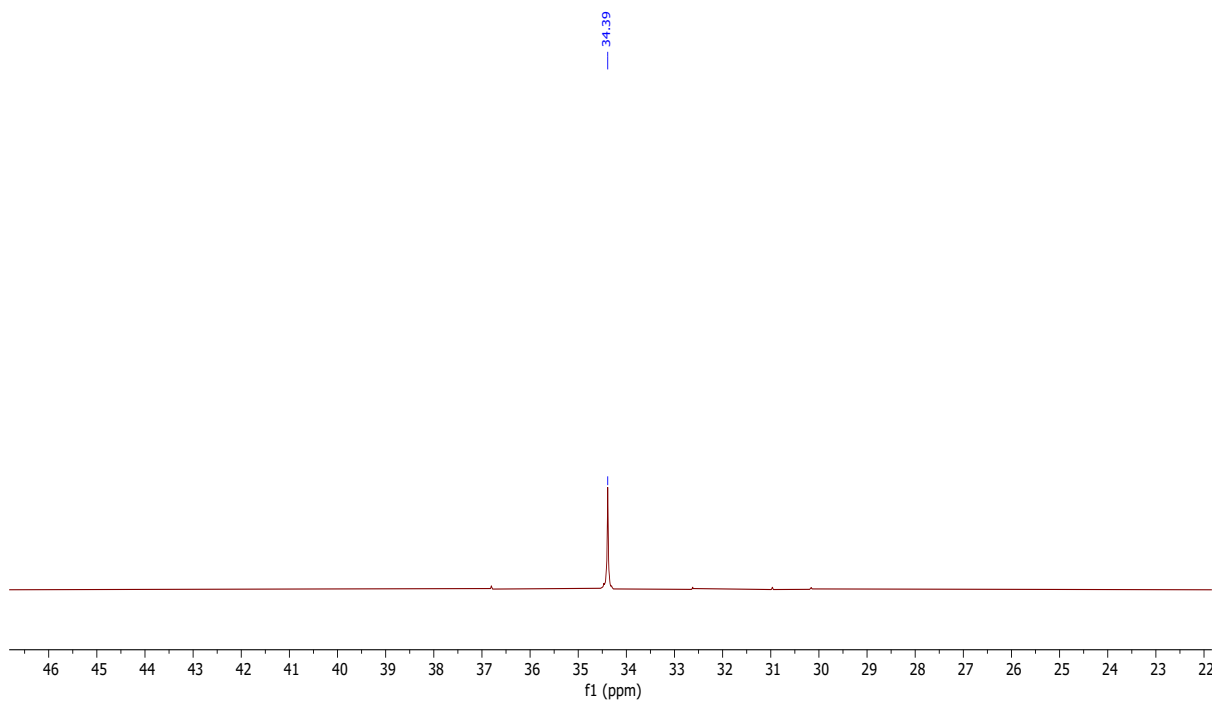
**Figure S8:**  $^{29}\text{Si}$ -NMR of  $\text{FR}_2$ .



**Figure S9:** HRMS spectrum of  $\text{FR}_2$ .



**Figure S10:** FTIR spectra of bDMVSiB, DPPO and FR<sub>2</sub>.

**Figure S11:** <sup>1</sup>H-NMR of FR<sub>3</sub>.**Figure S12:** <sup>31</sup>P-NMR of FR<sub>3</sub>.

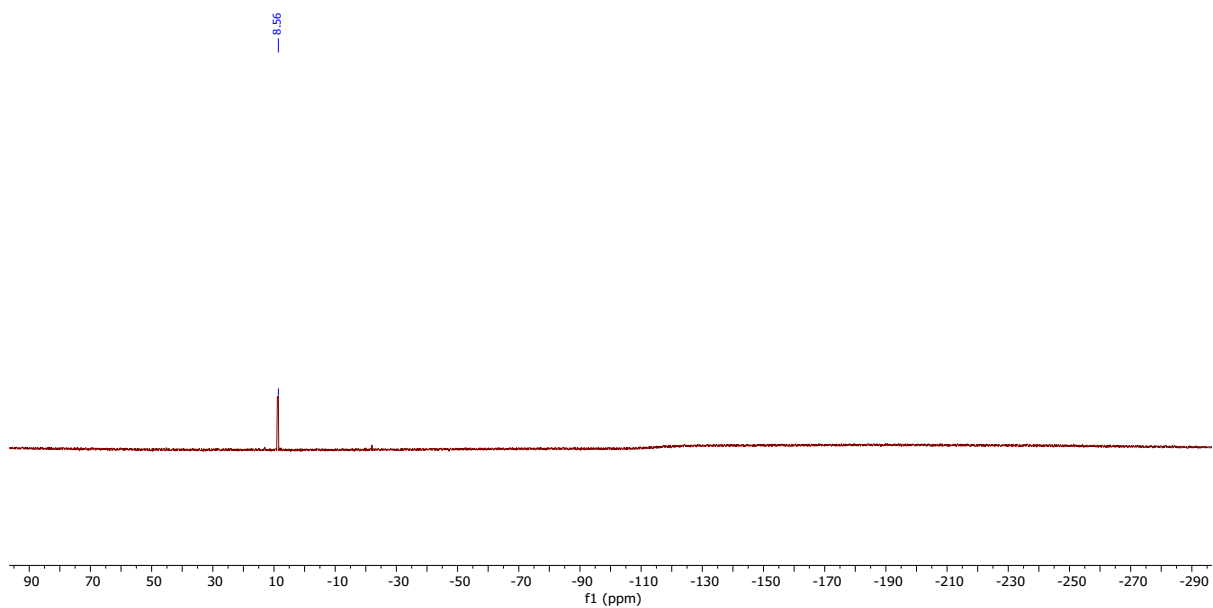


**Figure S13:**  $^{29}\text{Si}$ -NMR spectrum of FR<sub>3</sub>.

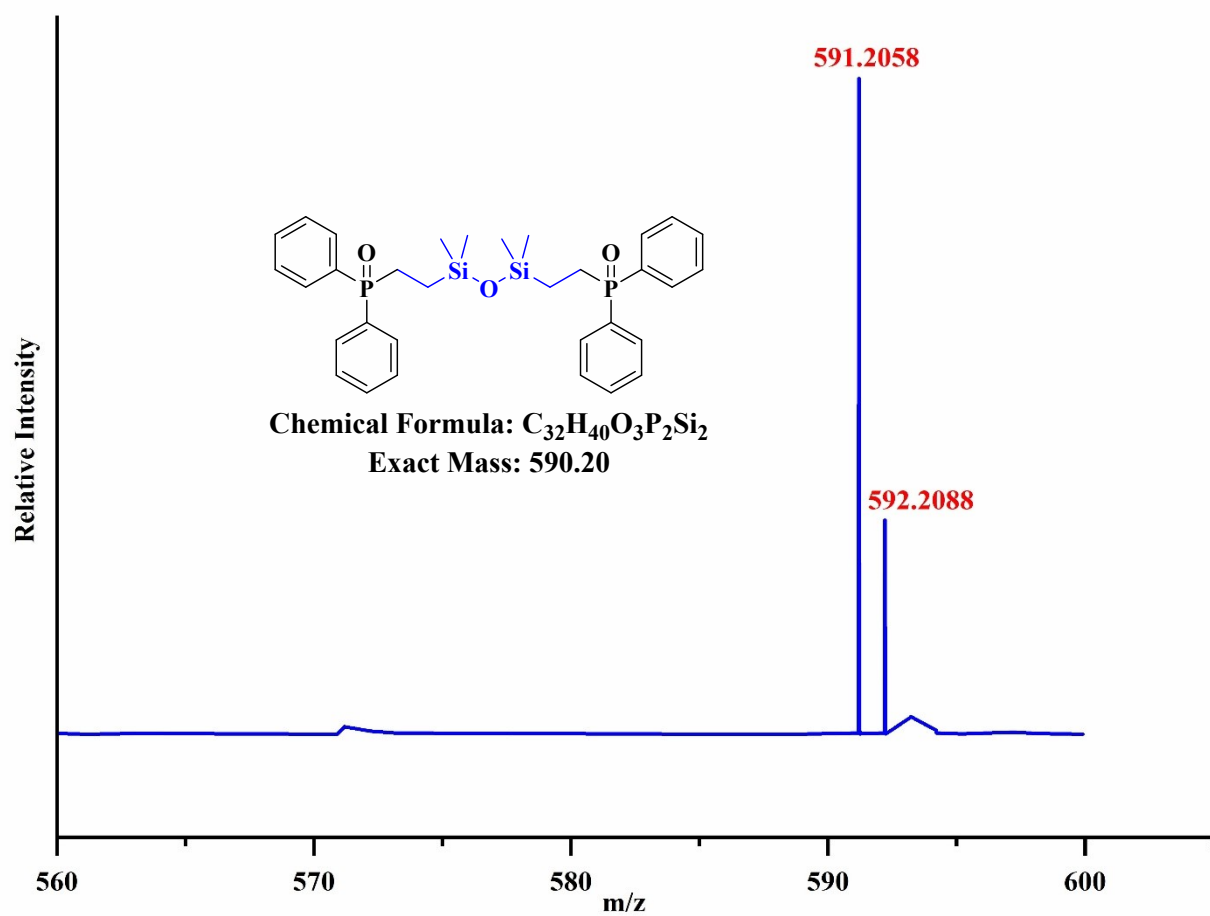


**Figure S14:** HRMS spectrum of FR<sub>3</sub>.

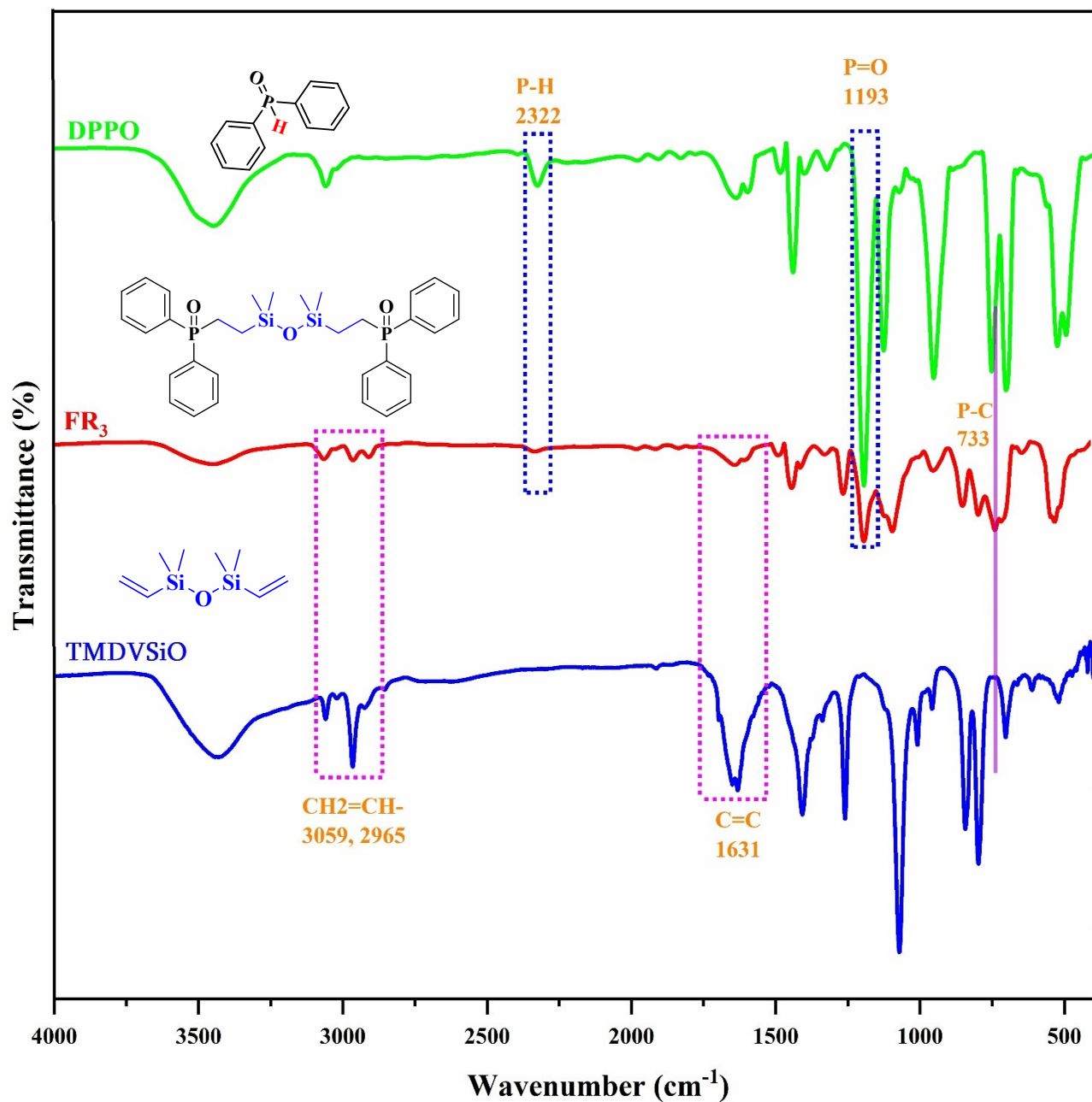
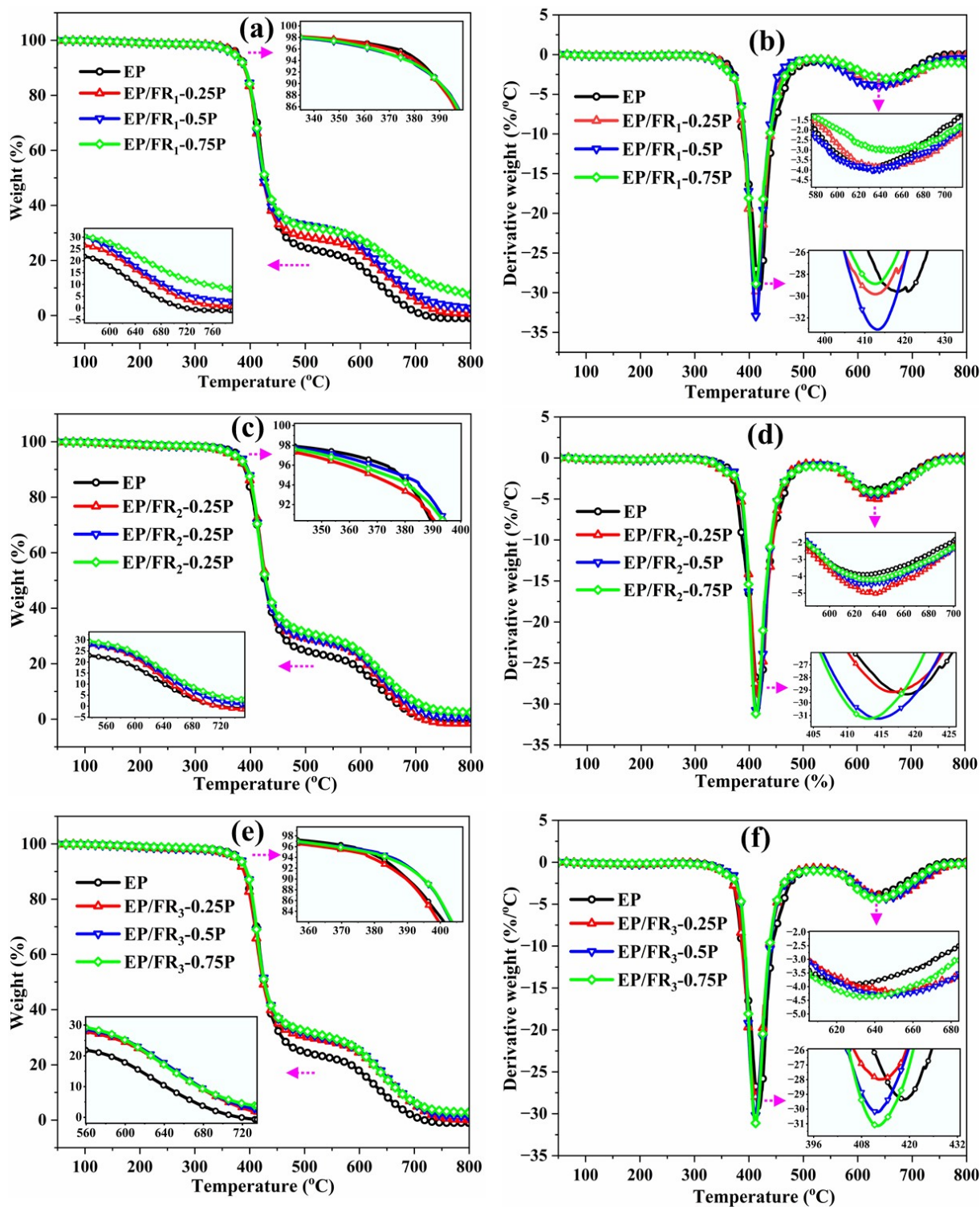


Figure S15: FTIR spectra of TMDVSiO, DPPO and FR<sub>3</sub>.



**Figure S16:** TGA and DTG curves of EP and EP/FR<sub>1</sub> (a, b), EP/FR<sub>2</sub> (c, d) and EP/FR<sub>3</sub> (e, f), composites under air atmosphere.

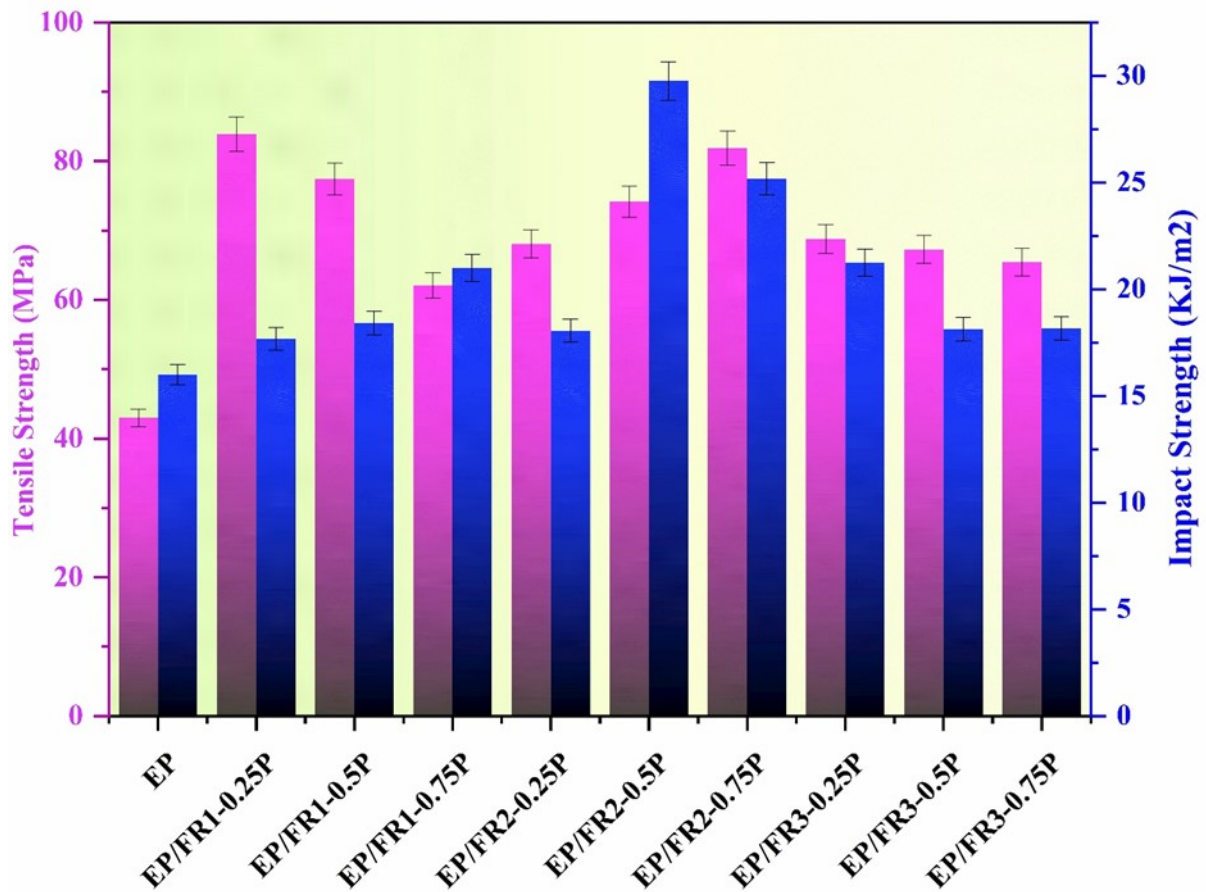


Figure S17: Tensile and impact strengths of different epoxy composites.

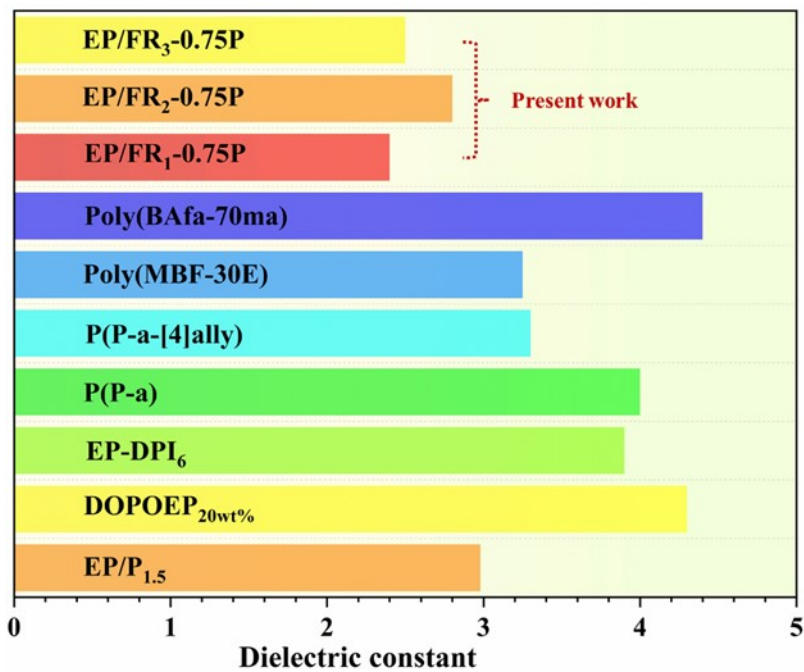
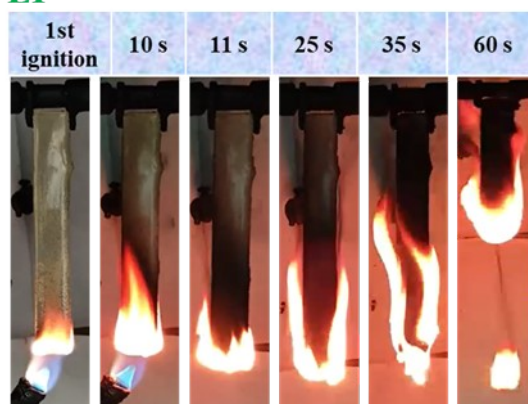


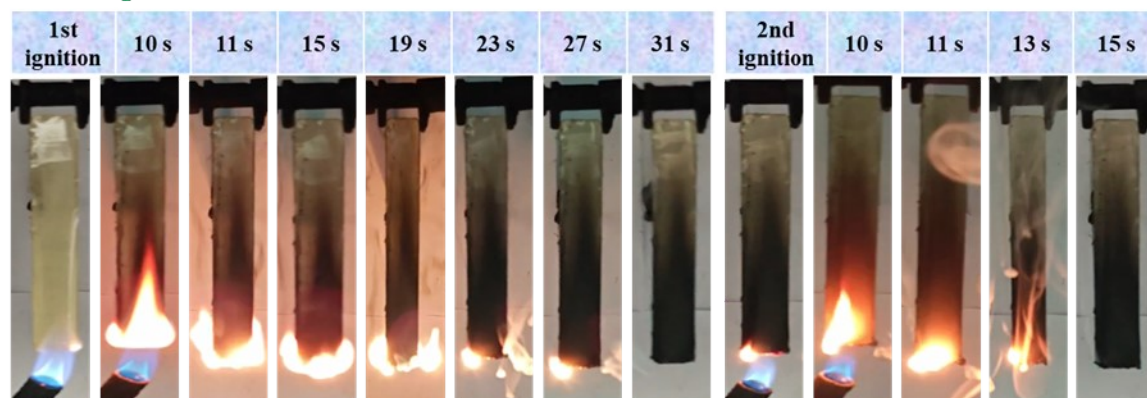
Figure S18: Comparison of the dielectric constant at 1 MHz frequency of the EP/FR composites of present work with the related literature.

**EP**

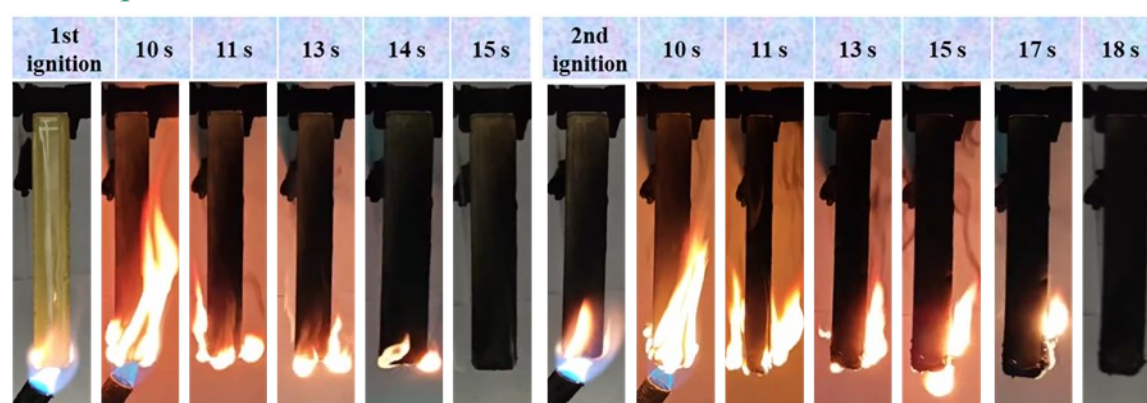


**Figure S19:** Real time digital photos of UL-94 vertical burning test of pure EP thermoset.

### EP/FR<sub>1</sub>-0.25P



### EP/FR<sub>1</sub>-0.5P



### EP/FR<sub>1</sub>-0.75P

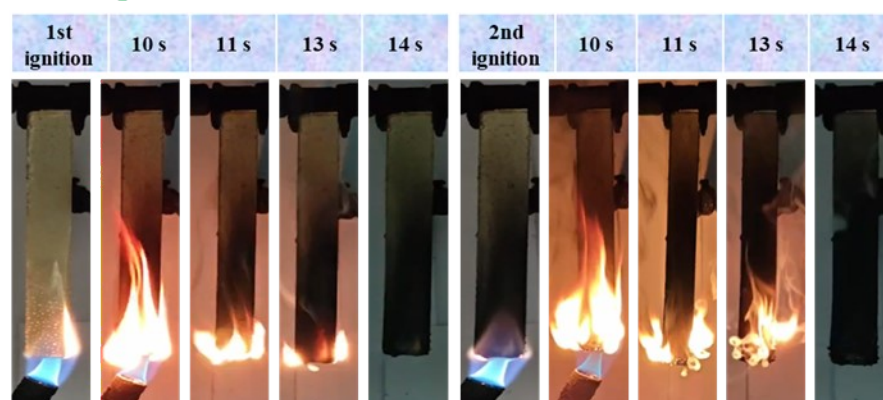
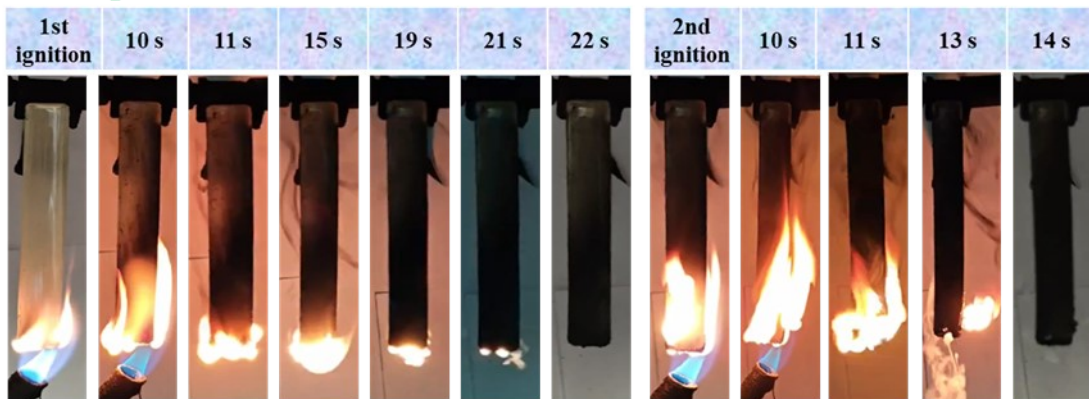
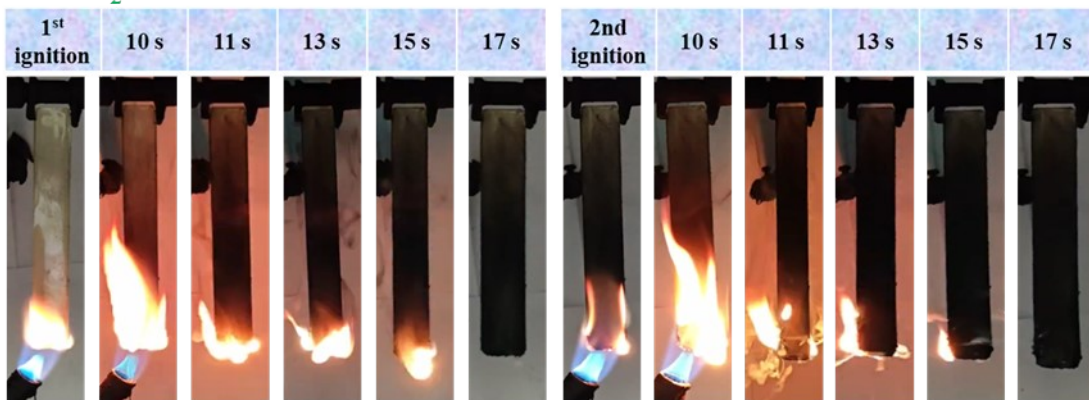


**Figure S20:** Real time digital photos of UL-94 vertical burning test of FR<sub>1</sub> epoxy thermosets at different P-content.

### EP/FR<sub>2</sub>-0.25P



### EP/FR<sub>2</sub>-0.5P



### EP/FR<sub>2</sub>-0.75P

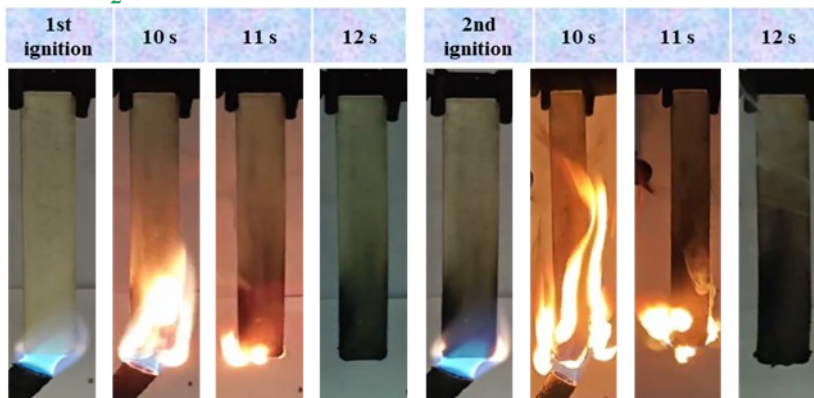
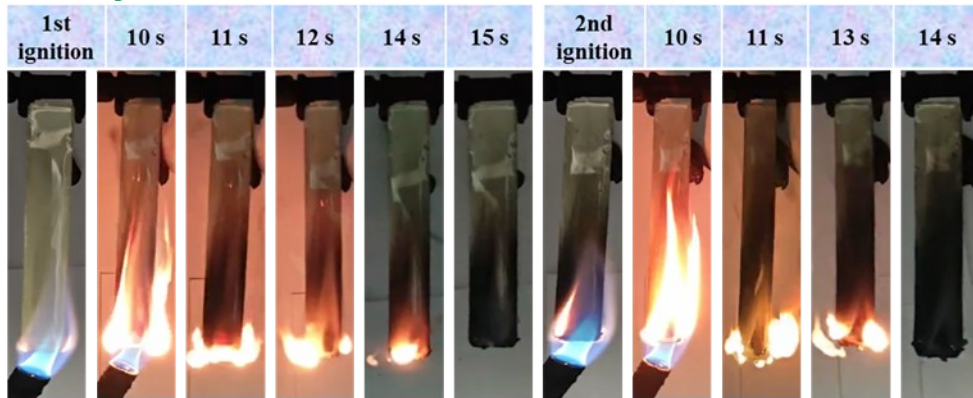
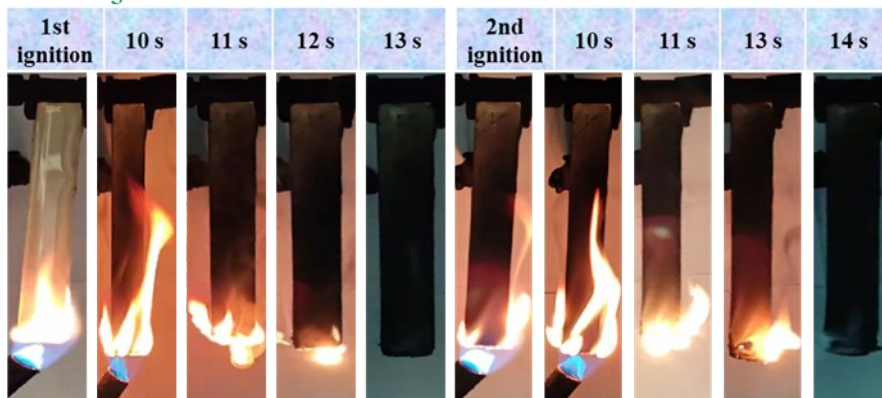


**Figure S21:** Real time digital photos of UL-94 vertical burning test of FR<sub>2</sub> epoxy thermosets at different P-content.

### EP/FR<sub>3</sub>-0.25P



### EP/FR<sub>3</sub>-0.5P



### EP/FR<sub>3</sub>-0.75P

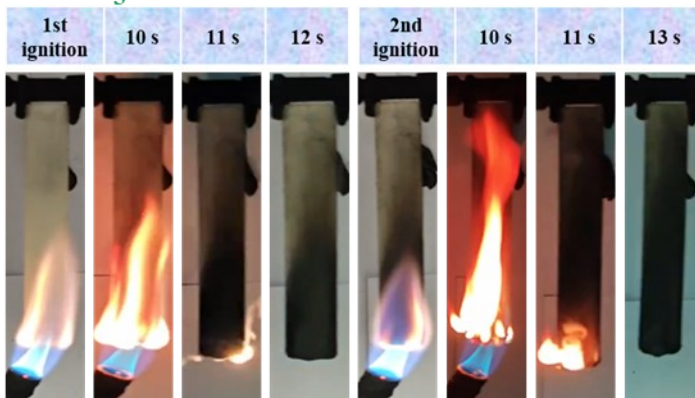


**Figure S22:** Real time digital photos of UL-94 vertical burning test of FR<sub>3</sub> epoxy thermosets at different P-content.

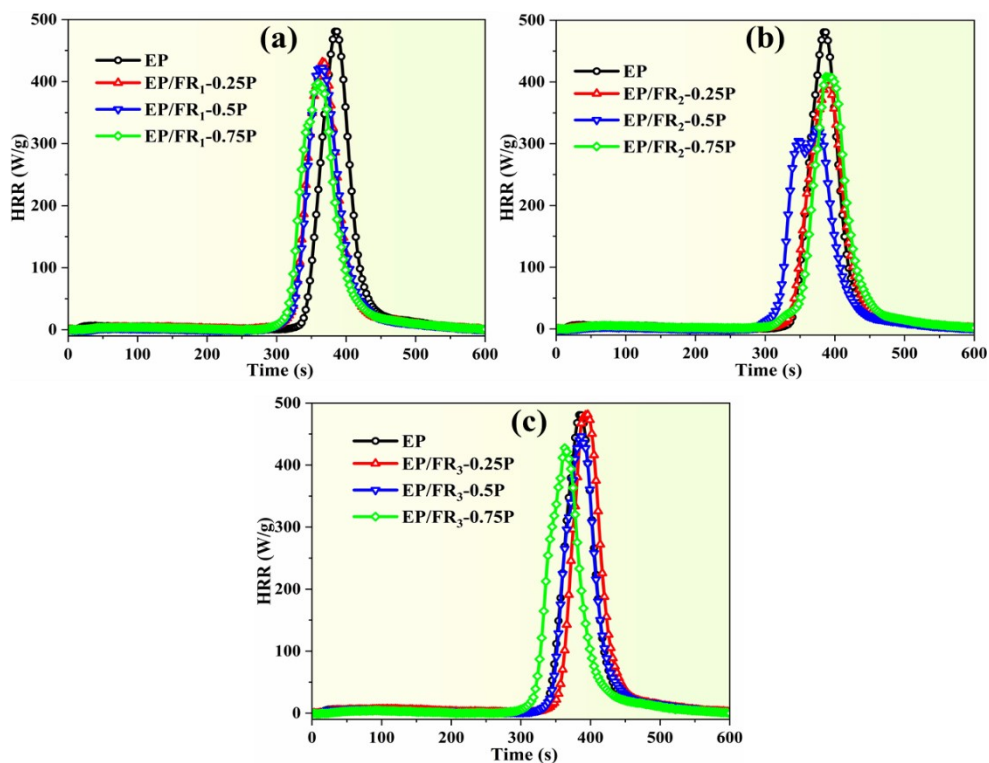


**Figure S23:** Comparison of MCC curves of pure EP with FR<sub>1</sub> (a), FR<sub>2</sub> (b), and FR<sub>3</sub> (c) epoxy thermosets at different phosphorous content.

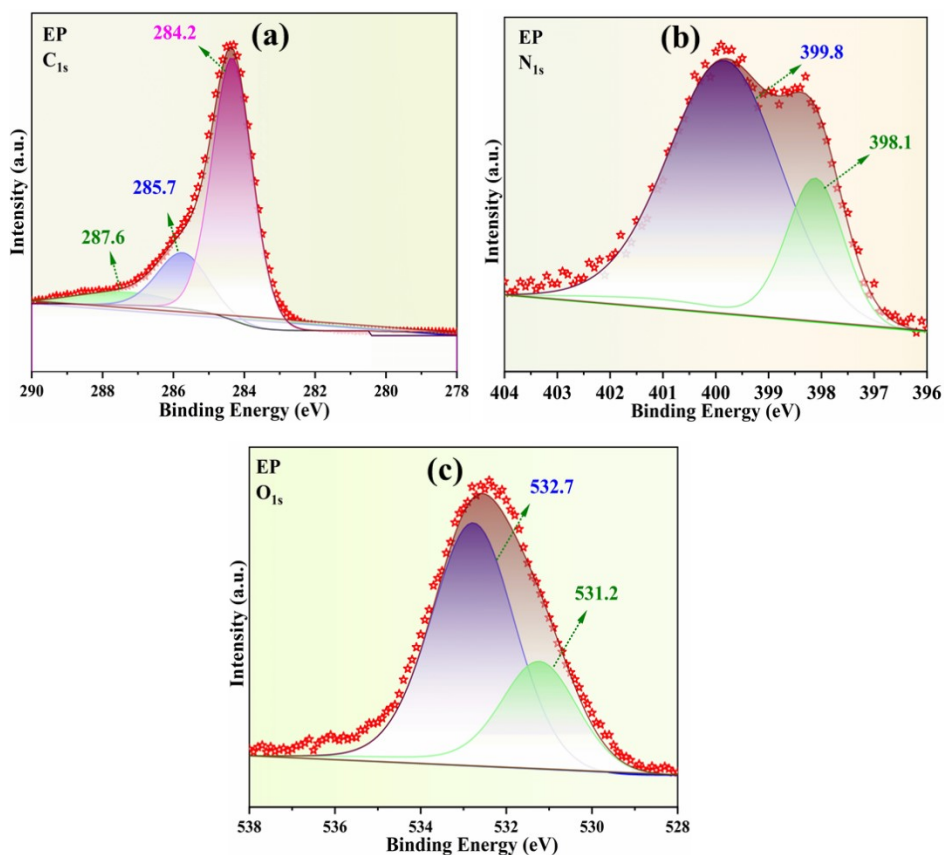


**Figure S24:** (a) C<sub>1s</sub>, (b) N<sub>1s</sub> and (c) O<sub>1s</sub>, XPS spectra for the char residue of EP.

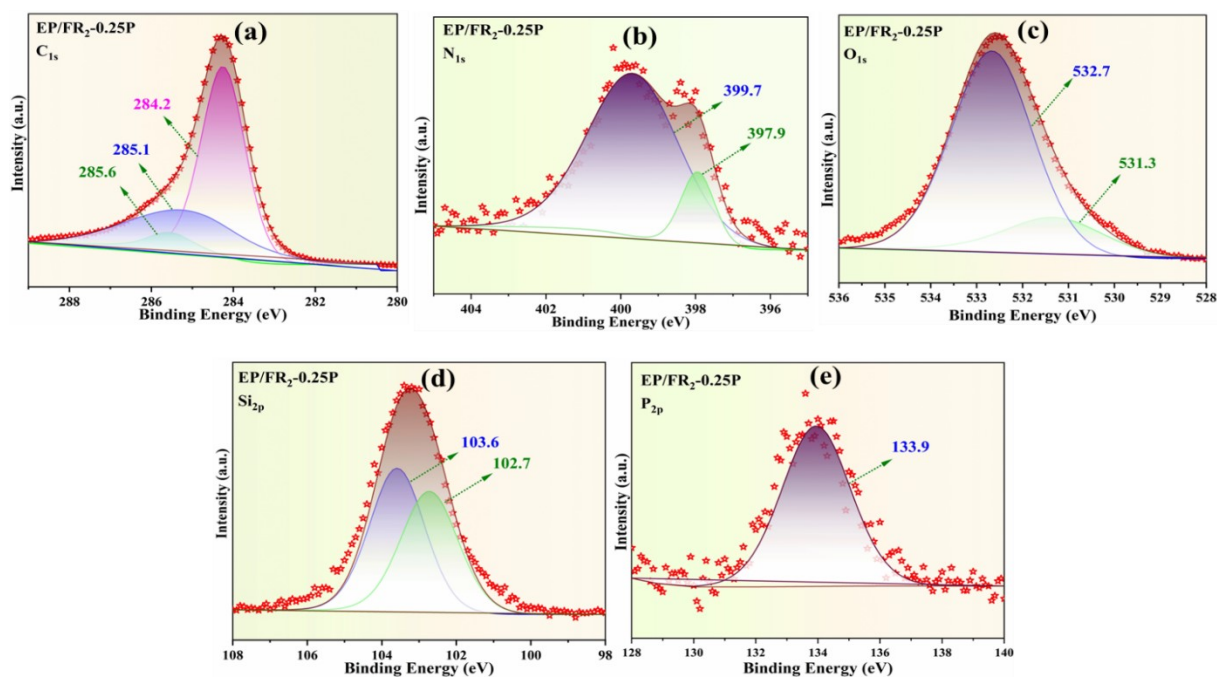


**Figure S25:** (a)  $C_{1s}$ , (b)  $N_{1s}$  and (c)  $O_{1s}$ , (d)  $Si_{2p}$  and (e)  $P_{2p}$  XPS spectra for the char residue of EP/FR<sub>2</sub>-0.25P.

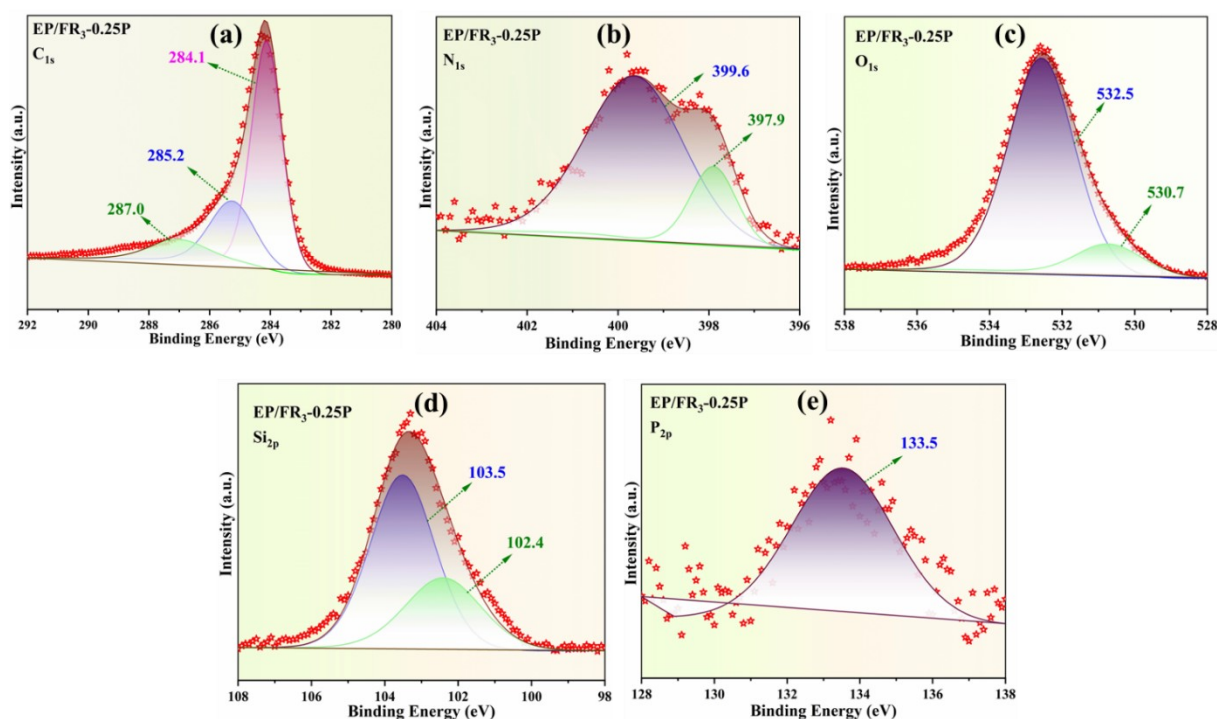


**Figure S26:** (a)  $C_{1s}$ , (b)  $N_{1s}$  and (c)  $O_{1s}$ , (d)  $Si_{2p}$  and (e)  $P_{2p}$  XPS spectra for the char residue of EP/FR<sub>3</sub>-0.25P.

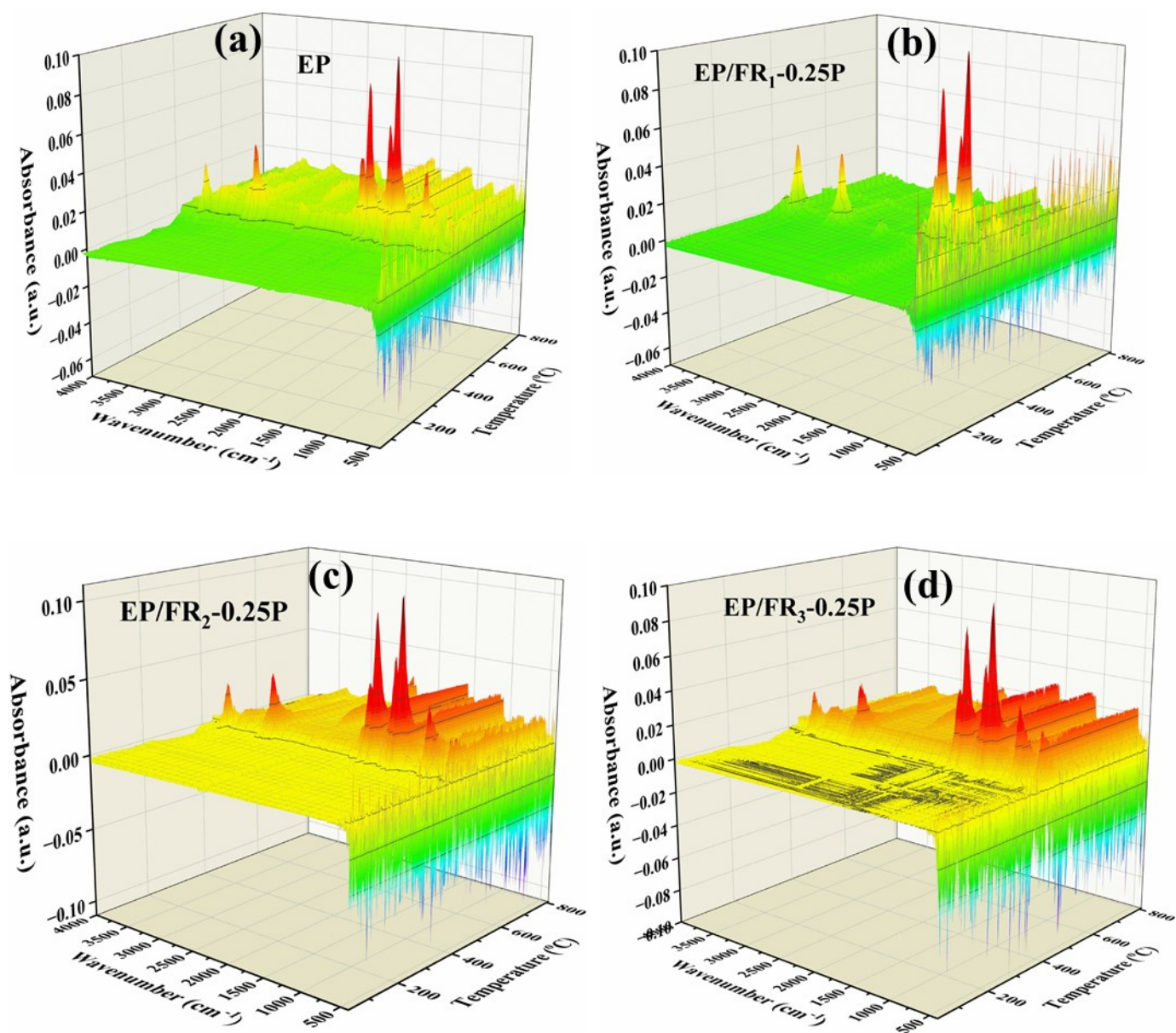


**Figure S27:** 3D TG-IR spectra of gaseous pyrolysis volatiles of (a) EP, (b) EP/FR<sub>1</sub>-0.25P, (c) EP/FR<sub>2</sub>-0.25P and (d) EP/FR<sub>3</sub>-0.25P.

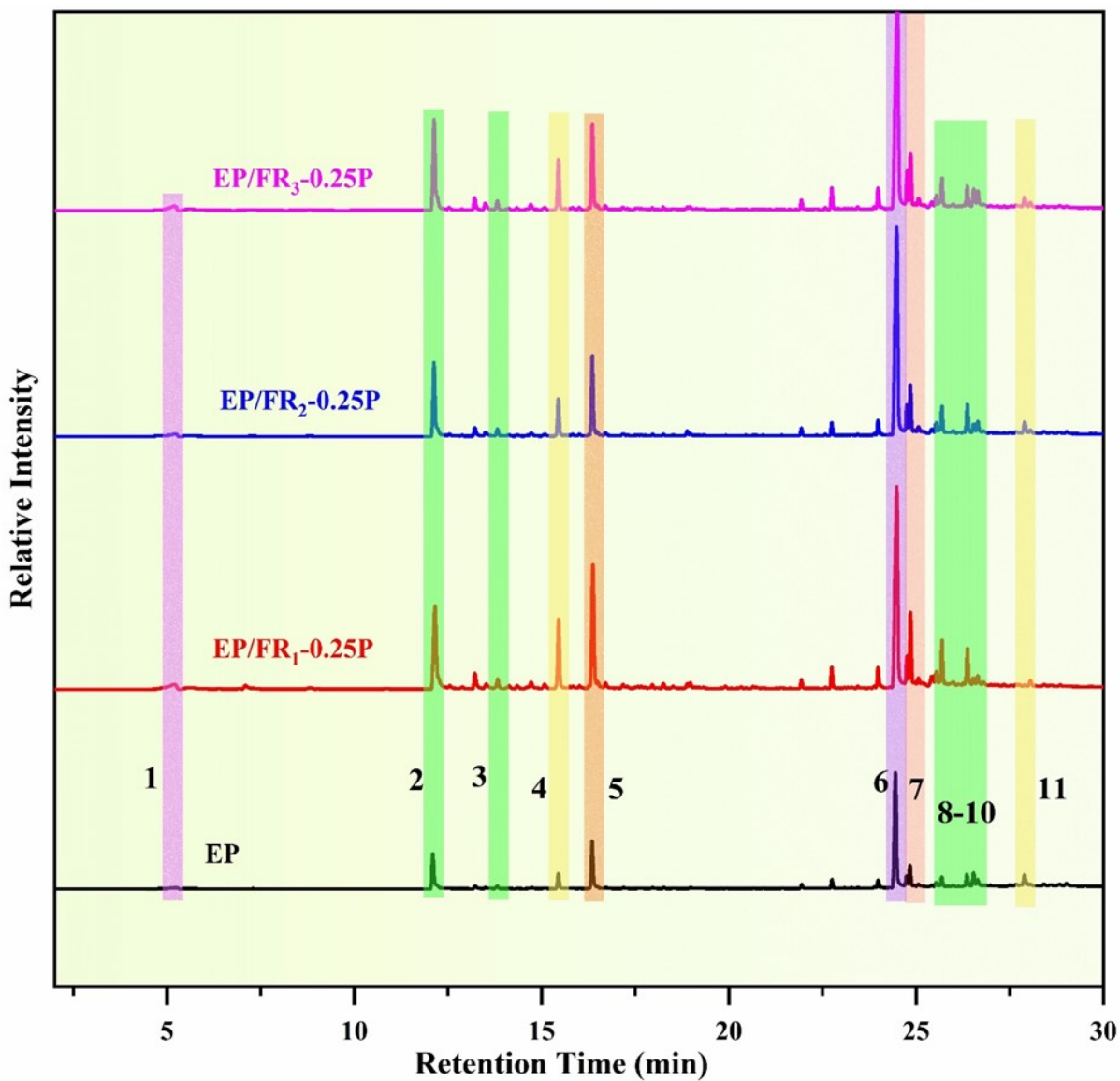


**Figure S28:** Comparison of TIC curve of EP and EP/FR<sub>1</sub>-0.25P, EP/FR<sub>2</sub>-0.25P, EP/FR<sub>3</sub>-0.25P composites.

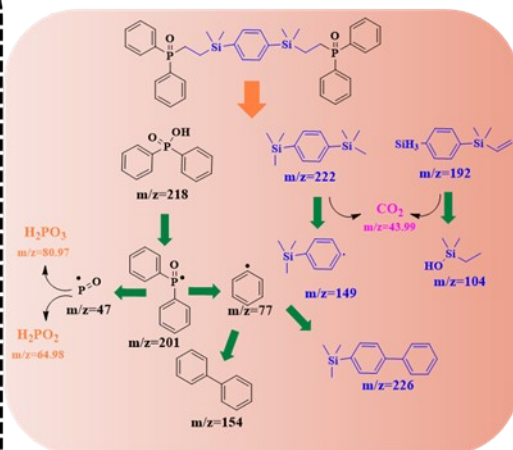
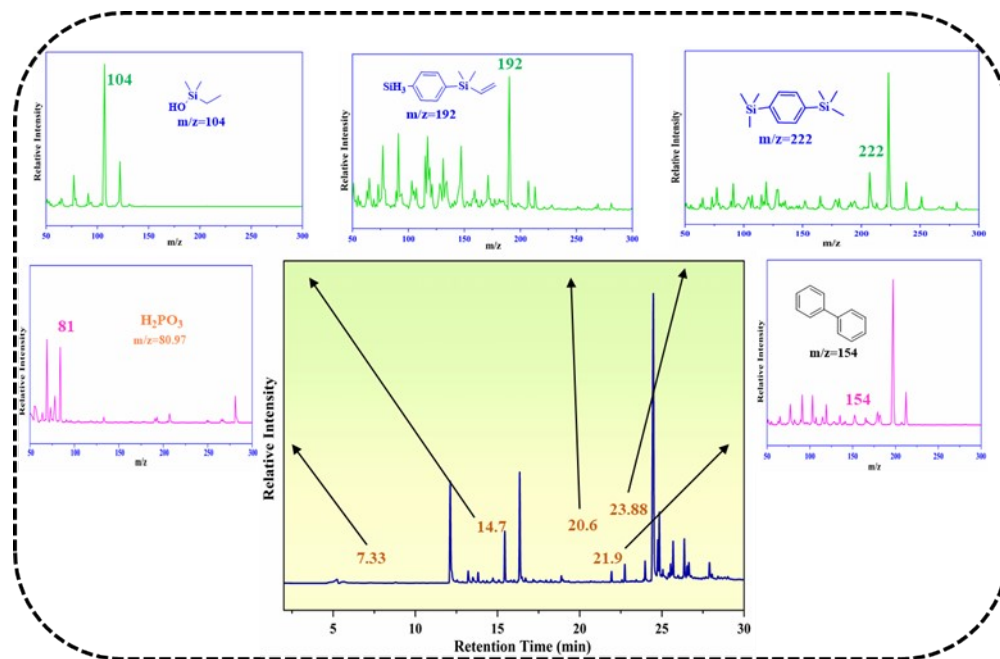


**Figure S29:** TIC curve along with the mass spectra of different fragments at their respective retention time and proposed pyrolysis pathway of the FR<sub>2</sub>.

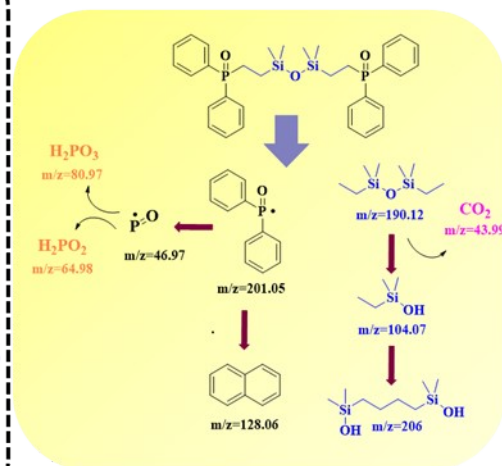
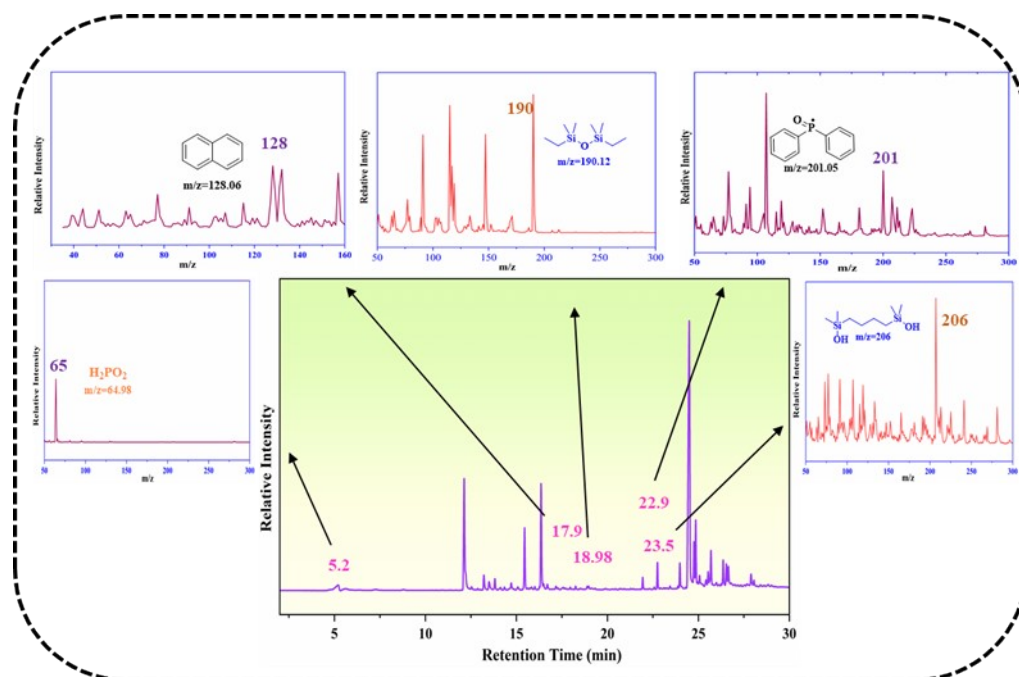


**Figure S30:** TIC curve along with the mass spectra of different fragments at their respective retention time and proposed pyrolysis pathway of the FR<sub>3</sub>.

Sample	T <sub>5%</sub> (°C)	T <sub>max1</sub> (°C)	T <sub>max2</sub> (°C)	R <sub>max1</sub> (%/°C)	R <sub>max2</sub> (%/°C)	Char residues (%)
EP	378	419	623	29.5	3.8	18.0
EP/FR <sub>1</sub> -0.25P	375	414	641	30.2	3.9	23.4
EP/FR <sub>1</sub> -0.5P	371	413	631	32.9	3.7	25.6
EP/FR <sub>1</sub> -0.75P	371	413	645	28.9	3.0	27.8
EP/FR <sub>2</sub> -0.25P	368	416	635	29.1	5.0	22.9
EP/FR <sub>2</sub> -0.5P	378	414	635	31.2	4.5	23.7
EP/FR <sub>2</sub> -0.75P	373	413	637	31.3	4.2	24.5
EP/FR <sub>3</sub> -0.25P	374	412	651	28.0	4.1	24.5
EP/FR <sub>3</sub> -0.5P	380	412	647	30.2	4.3	24.6
EP/FR <sub>3</sub> -0.75P	378	412	635	31.1	4.4	24.7

**Table S1:** TGA data of designed epoxy thermosets under air atmosphere.

Sample	T <sub>g</sub> (°C)	E' @ 30 °C (MPa)	E' @ T <sub>g</sub> +30 °C (MPa)	v <sub>e</sub> (mol/m <sup>3</sup> )	<b>Table S2:</b> DMA results of epoxy thermosets.
EP	199	1703.6	16.0	1277.5	
EP/FR <sub>1</sub> -0.25P	178	2055.9	12.4	1033.3	
EP/FR <sub>2</sub> -0.25P	192	1910.6	15.1	1384.6	
EP/FR <sub>3</sub> -0.25P	180	1941.1	15.3	1269.6	
EP/FR <sub>3</sub> -0.5P	175	1438.9	9.2	771.4	
EP/FR <sub>3</sub> -0.75P	169	1674.9	9.1	772.7	

**Table S3:** Tensile strength and impact strength of epoxy thermoset in previous research.

Sample	Tensile strength (MPa)	Impact strength (kJ/m <sup>2</sup> )	Reference
EP/DOPO-GL-DCDA-1.5P	74.45	29.99	[52]
EP/4DIT	46.7	10.02	[53]
EP-4	36.7	11.7	[54]
6NicNi@APP/EP	71.6	20.0	[55]
EP/ADIM-20	35.6	4.3	[56]
EP/MPD-12.5 %	50.8	4.9	[57]
EP/PDI-11 %	70.3	9.2	[58]
EP/GC@APP8	53.2	6.47	[59]

**Table S4:** Comparison of the dielectric constant at 1 MHz frequency for different epoxy thermosets in present work and other related literature.

Samples	Dielectric constant at 1 MHz	References
EP/P <sub>1.5</sub>	2.98	[63]
DOPOEP20wt%	4.3	[64]
EP-DPI6	3.9	[65]
P(P-a)	4.0	[65]
P(P-a-[4]allyl)	3.3	[66]

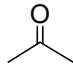
<b>Poly(MBF-30E)</b>	3.25	[67]
<b>poly(BAfa-70ma)</b>	4.4	[68]
<b>EP/FR<sub>1</sub>-0.75</b>	2.4	
<b>EP/FR<sub>2</sub>-0.75</b>	2.8	Present Work
<b>EP/FR<sub>3</sub>-0.75</b>	2.5	

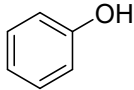
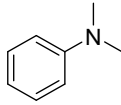
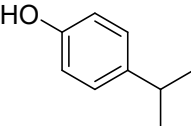
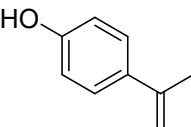
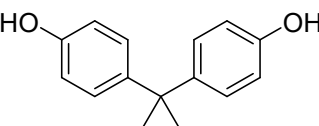
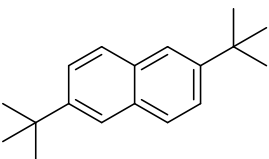
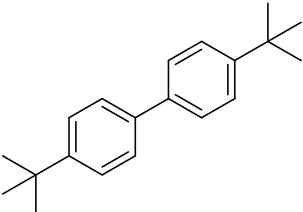
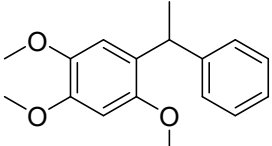
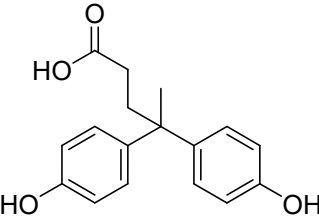
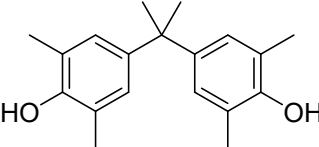
**Table S5:** Flame retardancy performance of the designed EP thermosets through cone

Sample	EP	EP/FR <sub>1</sub> -0.25P	EP/FR <sub>2</sub> -0.25P	EP/FR <sub>3</sub> -0.25P	EP/FR <sub>3</sub> -0.5P	EP/FR <sub>3</sub> -0.75P
<b>TTI (s)</b>	56	54	51	60	56	51
<b>PHRR (kW/m<sup>2</sup>)</b>	1096	849	731	819	701	621
<b>THR (MJ/m<sup>2</sup>)</b>	113.7	93.5	92.7	93.7	95.2	84.5
<b>TSP (m<sup>2</sup>)</b>	21.0	17.6	14.9	21.1	20.4	21.1
<b>av-CO<sub>2</sub>Y (kg/kg)</b>	4.5	5.6	5.0	4.6	4.6	4.8
<b>av-COY (kg/kg)</b>	0.223	0.469	0.334	0.294	0.296	0.369
<b>av-EHC (MJ/kg)</b>	30.6	31.7	29.8	29.9	28.3	30.3
<b>Residual Mass (%)</b>	4.4	8.4	4.5	8.8	13.2	11.2
<b>FRI</b>	1.00	1.52	1.67	1.73	1.9	2.16

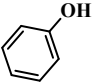
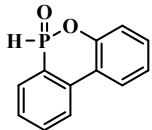
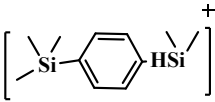
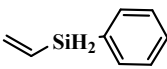
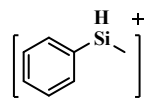
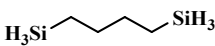
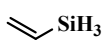
calorimetry.

**Table S6:** Identification of typical pyrolysis products for EP obtained from Py-GC/MS.

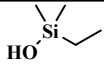
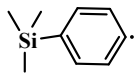
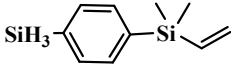
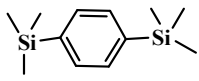
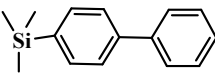
Peaks	Retention Time (min)	Structural formula	Molecular weight (m/z)
1	5.667		58.04

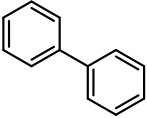
2	12.095		94.04
3	13.82		121
4	15.45		121.06
5	16.35		134.1
6	24.45		213.12
7	24.83		225.12
8	25.69		266.2
9	26.53		272.14
10	26.64		286.12
11	27.89		284.18

**Table S7:** Identification of typical pyrolysis products for EP/FR<sub>1</sub>-0.25P obtained from Py-GC/MS.

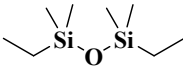
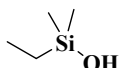
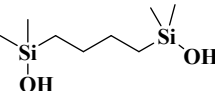
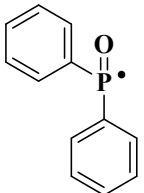
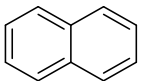
Peaks	Retention Time (min)	Structural formula	Molecular weight (m/z)
1a	12.16		94
2a	22.75		216
3a	28.02		207
4a	15		134
5a	20.7		121
6a	25.69		118
7a	5.52		58

**Table S8:** Identification of typical pyrolysis products for EP/FR<sub>2</sub>-0.25P obtained from Py-GC/MS.

Peaks	Retention Time (min)	Structural formula	Molecular weight (m/z)
1b	14.7		104
2b	17.2		149
3b	20.6		192
4b	23.88		222
5b	24.7		226

6b	27.9		154
7b	7.33	H <sub>2</sub> PO <sub>3</sub>	80.97

**Table S9:** Identification of typical pyrolysis products for EP/FR<sub>3</sub>-0.25P obtained from Py-GC/MS.

Peaks	Retention Time (min)	Structural formula	Molecular weight (m/z)
1c	18.98		190
2c	13.52		104
3c	23.5		206
4c	22.9		201
5c	17.9		128
6c	5.2	H <sub>2</sub> PO <sub>2</sub>	65